NASA TECHNICAL MEMORANDUM

NASA TM X-2955

NASA TM X-2955

OPERATING CHARACTERISTICS OF THE LANGLEY MACH 10 HIGH REYNOLDS NUMBER HELIUM TUNNEL

by Ralph D. Watson, Dana J. Morris, and Michael C. Fischer

Langley Research Center
Hampton, Va. 23665

NATIONAL AERONAUTICS AND SPACE ADMINISTRATION • WASHINGTON, D. C. • JUNE 1974

1. Report No. NASA TM X-2955	2. Government Accession No.	3. Recipient's Catalog No.
4. Title and Subtitle OPERATING CHARACTERISTICS OF THE LANGLEY MACH 10 HIGH REYNOLDS NUMBER HELIUM TUNNEL		5. Report Date June 1974 6. Performing Organization Code
7. Author(s) Ralph D. Watson, Dana J. Morris, and Michael C. Fischer		8. Performing Organization Report No. L-9259 10. Work Unit No. 501-06-08-01
9. Performing Organization Name and Address NASA Langley Research Center Hampton, Va. 23365		11. Contract or Grant No. 13. Type of Report and Period Covered Technical Memorandum
12. Sponsoring Agency Name and Address National Aeronautics and Space Administration Washington, D.C. 20546		14. Sponsoring Agency Code

15. Supplementary Notes

16. Abstract

Operating characteristics of the Langley Mach 10 high Reynolds number helium tunnel are presented for stagnation pressures from 138 N/cm^2 to 1655 N/cm^2. The characteristics include detailed Mach number surveys in the test section from which usable core size and regions of disturbed flow were determined, preliminary blockage test results, and maximum run time to be expected at various stagnation pressures. Important tunnel dimensions including details of the model mounting apparatus are given. Measurements show the variation in average core Mach number in the test section to be between 9.4 and 10 for the present range of test conditions. The core radius is from 23 cm to 31.5 cm, depending on stagnation pressure and axial location in the test section.

17. Key Words (Suggested by Author(s))	18. Distribution Statement
Tunnel calibration Hypersonic flow	Unclassified – Unlimited STAR Category 11

19. Security Classif. (of this report)	20. Security Classif. (of this page)	21. No. of Pages	22. Price*
Unclassified	Unclassified	39	$3.25

*For sale by the National Technical Information Service, Springfield, Virginia 22151

OPERATING CHARACTERISTICS OF THE LANGLEY MACH 10 HIGH REYNOLDS NUMBER HELIUM TUNNEL

By Ralph D. Watson, Dana J. Morris, and Michael C. Fischer
Langley Research Center

SUMMARY

Operating characteristics of the Langley Mach 10 high Reynolds number helium tunnel are presented for stagnation pressures from 138 N/cm^2 to 1655 N/cm^2. The characteristics include detailed Mach number surveys in the test section from which usable core size and regions of disturbed flow were determined, preliminary blockage test results, and maximum run time to be expected at various stagnation pressures. Important tunnel dimensions including details of the model mounting apparatus are given. Measurements show the variation in average core Mach number in the test section to be between 9.4 and 10 for the present range of test conditions. The core radius is from 23 cm to 31.5 cm, depending on stagnation pressure and axial location in the test section.

INTRODUCTION

The Mach 10 leg of the Langley high Reynolds number helium tunnels is a unique facility capable of simulating flight Reynolds numbers in the hypersonic range. For example, figure 1 shows the Mach number-Reynolds number trajectory of a space shuttle (33.7-m-long) configuration, the cruise trajectory of a hypersonic airplane (24.4 m long), and the simulation range of the Mach 10 tunnel. On a relatively small 25.4-cm model, the Mach 10 section of both trajectories can be covered in this tunnel simply by varying stagnation pressure. Models up to more than a meter in length can be tested, the size depending on the fineness ratio, nose bluntness, and angle-of-attack range desired. A maximum Reynolds number of 222×10^6 can be obtained on a model 1 meter long.

The facility was designed to operate at a maximum stagnation pressure of 2755 N/cm^2 and stagnation temperatures up to 617 K. (See ref. 1.) Early problems with

a gas-fired heater were so great that the tunnels could be run efficiently only when the heater was removed from the system. Thus, at present, the flow is unheated. Although removal of the heater has made heat-transfer tests more difficult since the model must be cooled to produce low ratios of wall temperature to total temperature, the overall research capability of the facility has not been degraded. For example, instrumentation problems are reduced when operating at ambient stagnation temperature for instruments such as skin-friction balances, hot wires, and many types of pressure transducers. Also, unheated Mach 10 helium flow is an excellent test medium to provide data for checking viscous-shear-flow calculation programs currently being developed. The largest density ratio across the boundary layer, and thus the most stringent test cases, are obtained at ratios of wall temperature to total temperature near 1.

Both the Mach 10 and Mach 20 legs of the high Reynolds number helium tunnels can operate at stagnation pressures as high as 2755 N/cm^2; however, it becomes impractical to operate the Mach 10 leg at the higher stagnation pressures because of limited vacuum sphere and high-pressure-supply volume. Operating experience has shown that a practical upper limit is about 1655 N/cm^2; accordingly, the tunnel has been calibrated to this pressure.

This report contains detailed Mach number distributions in the Mach 10 leg for stagnation pressures from 138 N/cm^2 to 1655 N/cm^2 which covers a unit Reynolds number range from 10.8×10^6 to 133.6×10^6 per meter. Total temperature was between 230 K and 322 K for these runs. In addition to determining the Mach number distribution in the test section for a range of stagnation pressures, preliminary blockage tests were made at one location and the maximum tunnel run time was obtained.

SYMBOLS

D	test-section diameter
M	free-stream Mach number
$\overline{M}$	average Mach number

p	pressure
R_l	Reynolds number based on length
r	radial tunnel coordinate
r_c	inviscid core radius
T	temperature
x	axial tunnel distance, measured from nozzle throat
$\bar{x}$	axial tunnel distance, measured from station 186.61
δ	boundary-layer pitot thickness
δ^*	boundary-layer displacement thickness
ϕ	angular coordinate (see fig. 6)

Subscripts:

t	total value
w	wall
∞	free-stream value

DESCRIPTION OF FACILITY

The Langley high Reynolds number helium tunnels consist of Mach 10 and Mach 20 legs connected to common high-pressure storage tanks with a volume of 56.6 m^3 and to vacuum spheres with a volume of 6526 m^3. A schematic diagram of the facility is shown in figure 2. Operating characteristics of the Mach 20 leg can be found in reference 2.

Figure 3 shows the components and important dimensions of the Mach 10 leg. In figure 3(a) the overall tunnel dimensions are shown from the pressure control valve to the sphere isolation valve downstream of the diffuser. The diffuser is a fixed-area design having a ratio of minimum area to test-section area of 0.83. Details of the test section are shown in figure 3(b). A cross-section view shows the four removable plates that give access to the test section. The two side plates are of optical-quality glass for schlieren studies and all plates are interchangeable.

Models can be sting mounted on the hydraulically driven, programmable arc mechanism or from the floor of the tunnel. Since the test section diverges 0.683° downstream, a set of leveling wedges has been attached to the floor of the tunnel for strut-mounting models in any part of the test section. Figure 4 is a photograph of the test section.

Details of the axisymmetric contoured nozzle are shown in figure 5. For a stagnation pressure of 2758 N/cm^2 and $T_w = T_t = 294.3$ K, the turbulent wall displacement thickness δ^* was calculated by the method of reference 3. The displacement thickness is added to an inviscid core calculated by the method of characteristics to give the wall coordinates. The test section diverges at an angle of 0.683° downstream of the cutoff point. Also shown in the figure are details of the nozzle throat and experimental values of δ in the test section determined from the data of this report.

INSTRUMENTATION AND DATA REDUCTION

Pitot surveys were made at four axial locations in the test section using the two rakes shown in figure 6. The larger rake contained 32 tubes on 8 arms plus a center-line tube. Tube spacing was 10.2 cm on this rake. The smaller rake contained 20 tubes on 4 arms plus a center-line tube as well as 9 tubes arranged to provide a coarse pressure distribution within the tunnel-wall boundary layer. Tube spacing on this rake was 2.54 cm.

Pressures were measured by using strain-gage transducers calibrated to one-quarter percent accuracy of full-scale output. Different ranges of transducers were used to provide maximum accuracy. It is estimated that all pressures are measured to better than 1 percent of the true value. Tunnel total temperature was measured with a bare-wire iron-constantan thermocouple in the stagnation chamber.

Data were recorded on tape in digital form. Mach numbers were calculated from pitot and stagnation pressure by two different methods. Data from the center tubes of the

small rake (see fig. 6) as well as all data from the large rake were reduced by assuming isentropic nozzle flow. Mach numbers were calculated from equation (15) of reference 4. Within the tunnel-wall boundary layer, isentropic expansion from stagnation conditions cannot be assumed. On the boundary-layer arm, the average Mach number was determined by using static pressures calculated from core data along with the measured local pitot pressure. By assuming the static pressure to be constant through the boundary layer, Mach numbers were calculated by use of the Rayleigh pitot formula (eq. (16) of ref. 4). For both reductions the real-gas corrections of reference 5 were used.

RESULTS AND DISCUSSION

At Mach numbers representative of the highest and lowest stagnation pressures of the calibration and for values of T_t representative of these stagnation conditions, the following flow parameters of interest have been calculated by using the real-gas correction factors of reference 5:

Stagnation conditions:		
p_t, N/cm^2	137.9	1585.9
T_t, K	289.9	255.6
Mach number	9.4	10
Static pressure, N/cm^2	0.0393	0.3604
Static temperature, K	17.2	14.0
Dynamic pressure, N/cm^2	2.892	30.037
Velocity, m/sec	1708	1640
Unit Reynolds number/m	10.8×10^6	133.6×10^6

Starting transients in the high Reynolds number helium tunnels last about 1 second. During this time the stagnation pressure changes from tunnel vacuum to the desired level smoothly with no significant overshoot. However, the total temperature momentarily reaches a higher level during the starting process. Sketch (a) shows a simple schematic of the high-pressure reservoir, pressure control valve, stagnation chamber, and nozzle. Helium is throttled from a typical pressure of 3450 N/cm^2 in the supply line to a lower pressure in the stagnation chamber. The Joule-Thompson effect at the pressure-control valve produces a slight increase in T_t, about 15 K; however, a much larger effect is produced as the stagnation chamber is filled. In reference 6 this thermodynamic process is shown to produce a ratio of final to initial temperature equal to 1.67 for helium.

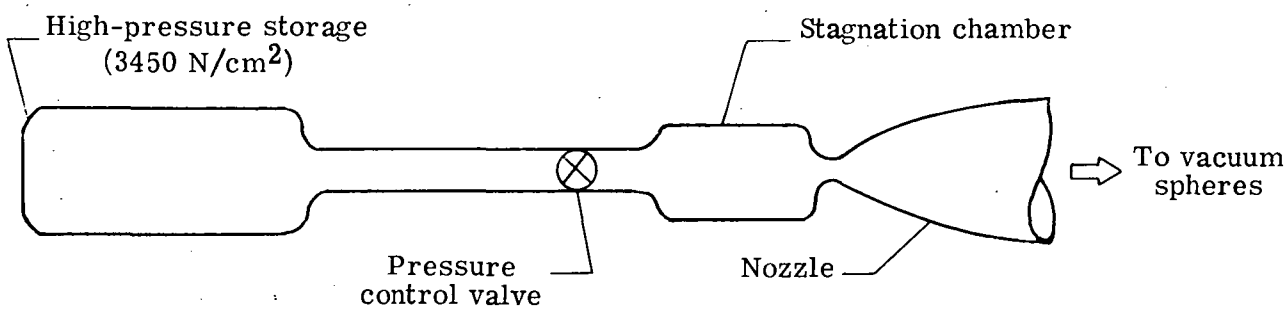

Sketch (a)

Figure 7 shows typical total-temperature histories for two different stagnation pressures. The data were recorded on a system containing filters to remove 60-Hz noise; thus, the true peak in T_t is not recorded. The large overshoot is evident as well as the rather slow return to near-ambient total temperature. During the run significant mass can be removed from the storage bottle; as a result, an almost linear decrease in total temperature with time is produced as the remaining helium expands. Despite the continual change in total temperature during a run, no time variation in free-stream Mach number could be detected at constant stagnation pressure.

Mach Number Distribution

Mach number surveys were made at $\bar{x}$ locations of 25.4, 76.2, 127, and 177.8 cm for nominal stagnation pressures of 138, 276, 414, 827, 1241, and 1655 N/cm^2. Data from the small rake are plotted in figure 8 as radial Mach number distributions. In general, the figure shows the flow to be symmetrical about the tunnel center line with disturbances in the immediate vicinity of the center line. The magnitude of the disturbance varies with axial location in the test section and with tunnel stagnation pressure. The disturbance region extends radially about 5 cm, although in most cases, the Mach number deviation is small beyond 1 cm. Measured pitot pressures were lower on the center line than for adjacent tubes, and produced peaks in Mach number when reduced, isentropic flow in the core being assumed.

Similar disturbances in a Mach 8 air tunnel (ref. 7) were traced to imperfections of about 0.013 cm in the nozzle wall. The effect whereby wall-induced disturbances in axisymmetric flow increase in magnitude toward the center line (the "radial focusing effect") is discussed in reference 8.

Center-line disturbances were stated in reference 9 to have negligible effect on the overall forces on a test body and little effect on the pressure distribution over slender bodies. Pressure and heat-transfer distributions on blunt bodies were significantly affected by disturbances when tested on the center line. The same trends will undoubtedly be found in the high Reynolds number Mach 10 tunnel and should be considered when the models are located in the test section.

Average Mach numbers were obtained by fairing the data of figure 8 between radii of 5 and 15 cm from the center line. Variation of the resulting average Mach number with tunnel stagnation pressure is shown in figure 9. The average core Mach number increases approximately proportional to the logarithm of the stagnation pressure. Figure 10 shows the Mach number variation with distance $\bar{x}$ in the test section. At a fixed stagnation pressure the Mach number change from the front to the rear of the test section is less than 0.16.

Data from the large rake are shown in figure 11 along with core data and boundary-layer arm data from the small rake. The outer tubes of the large rake are within the tunnel-wall boundary layer, and thus data for these tubes are omitted. Note that the lower and upper plots of each figure are not to the same scale. Data from the lower part of this figure were used to find the edge of the usable test core for each run. The core radius at each of the four survey stations is shown in figure 12 and figure 5.

Blockage Test

In order to determine the approximate model sizes which can be tested in the tunnel, starting tests with hemisphere cylinders of various diameters were made at $\bar{x}$ about 70 cm. The floor of the test section and the diffuser sidewall were instrumented with pressure transducers to determine whether potentially dangerous static pressures occurred downstream of the nozzle when an unstarted tunnel condition existed.

Tests were begun with a 24-cm-diameter model; the tunnel would not start at stagnation pressures of 138 N/cm^2 and 276 N/cm^2. The model size was reduced to 21.6 cm and blockage again occurred at these stagnation pressures. The model diameter was reduced to 18 cm and again the flow did not start. A further reduction of the model diameter to 12.4 cm allowed the tunnel to start at a stagnation pressure of 140 N/cm^2. Figure 13 shows the model to scale in the test section along with pressures measured on

the floor of the test section. The measured edge of the inviscid core from figure 11 is shown as well as shock shapes calculated by the method of reference 10 for spherical-nose bodies.

It was impossible to determine whether the flow was started from schlieren observations of the shock. The flow field appeared to be steady even when the flow was known to be blocked. From figure 13, wall pressures are indicative of a Mach 5 start, and it can be seen that calculated Mach 5 and Mach 10 shock shapes are not greatly different. It appears that when model blockage is too high, the tunnel-wall boundary layer separates upstream to the point where approximately Mach 5 flow is reached. When the tunnel flow is started, the wall static pressures are in agreement with the expected level.

Tunnel Run Time

By using the hemisphere-cylinder described in the preceding section, tunnel run time was established by running until natural flow breakdown occurred because of high backpressure in the vacuum spheres or until stagnation pressure dropped because of limited supply pressure. Figure 14 shows the results of these tests. Also shown is the calculated time limit at which the two vacuum spheres would reach atmospheric pressure, a condition at which automatic tunnel shutdown occurs since the spheres were not designed for an internal pressure above atmospheric.

At a stagnation pressure of approximately 300 N/cm^2, a sharp decrease in tunnel run time is evident, probably caused by a change in flow conditions within the diffuser. Above 300 N/cm^2, the tunnel run time decreases steadily with increasing stagnation pressure. At about 1200 N/cm^2, the pressure contained in one supply bottle is not sufficient to maintain constant stagnation pressure until flow breakdown is reached. Another supply bottle is available for high-pressure storage; however, it is usually not fully pressurized and is used to store impure helium for later purification. Optimum operation of both Mach 20 and Mach 10 tunnels is achieved by this arrangement.

CONCLUDING REMARKS

The Mach 10 leg of the Langley high Reynolds number helium tunnels has been calibrated for stagnation pressures from 138 N/cm^2 to 1655 N/cm^2. Mach number distributions at four positions within the test section are presented along with the results of a

flow-blockage test and the determination of tunnel run time within the range of calibration stagnation pressures.

In summary, four general characteristics of the flow can be noted as follows:

1. Pitot surveys indicate an average core Mach number variation from 9.4 to 10 at corresponding unit Reynolds numbers of 10.8×10^6 to 133.6×10^6 per meter.

2. The radius of the inviscid core ranges from 23 to 31.5 cm depending on stagnation pressure and test-section location.

3. Tunnel run time varies from about 16 seconds to about 3 seconds, depending on stagnation pressure.

4. A preliminary blockage test at one test-section location has shown that a spherically blunted, 12.4-cm-diameter body will start at a tunnel stagnation pressure of 138 N/cm^2; a model 18 cm in diameter will not start at this pressure.

Langley Research Center,
National Aeronautics and Space Administration,
Hampton, Va., February 13, 1974.

REFERENCES

1. Schaefer, William T., Jr.: Characteristics of Major Active Wind Tunnels at the Langley Research Center. NASA TM X-1130, 1965.

2. Watson, Ralph D.; and Bushnell, Dennis M.: Calibration of the Langley Mach 20 High Reynolds Number Helium Tunnel Including Diffuser Measurements. NASA TM X-2353, 1971.

3. Persh, Jerome; and Lee, Roland: A Method for Calculating Turbulent Boundary Layer Development in Supersonic and Hypersonic Nozzles Including the Effects of Heat Transfer. NAVORD Rep. 4200 (Aeroballistic Res. Rep. 320), U.S. Navy, June 7, 1956.

4. Mueller, James N.: Equations, Tables, and Figures for Use in the Analysis of Helium Flow at Supersonic and Hypersonic Speeds. NACA TN 4063, 1957.

5. Erickson, Wayne D.: Real-Gas Correction Factors for Hypersonic Flow Parameters in Helium. NASA TN D-462, 1960.

6. Dodge, Barnett F.: Chemical Engineering Thermodynamics. McGraw-Hill Book Co., Inc., 1944.

7. Fitch, C. R.: Flow Quality Improvement at Mach 8 in the VKF 50-Inch Hypersonic Wind Tunnel B. AEDC TR-66-82, U.S. Air Force, May 1966.

8. Meyer, R. E.: The Method of Characteristics for Problems of Compressible Flow Involving Two Independent Variables. Part II. Integration Along a Mach Line. The Radial Focusing Effect in Axially Symmetric Flow. Quart. Jour. Mech. and Appl. Math., vol. I, pt. 4, Dec. 1948, pp. 451-469.

9. Sivells, James C.: Aerodynamic Design and Calibration of the VKF 50-Inch Hypersonic Wind Tunnels. AEDC-TDR-62-230, U.S. Air Force, Mar. 1963.

10. Lomax, Harvard; and Inouye, Mamoru: Numerical Analysis of Flow Properties About Blunt Bodies Moving at Supersonic Speeds in an Equilibrium Gas. NASA TR R-204, 1964.

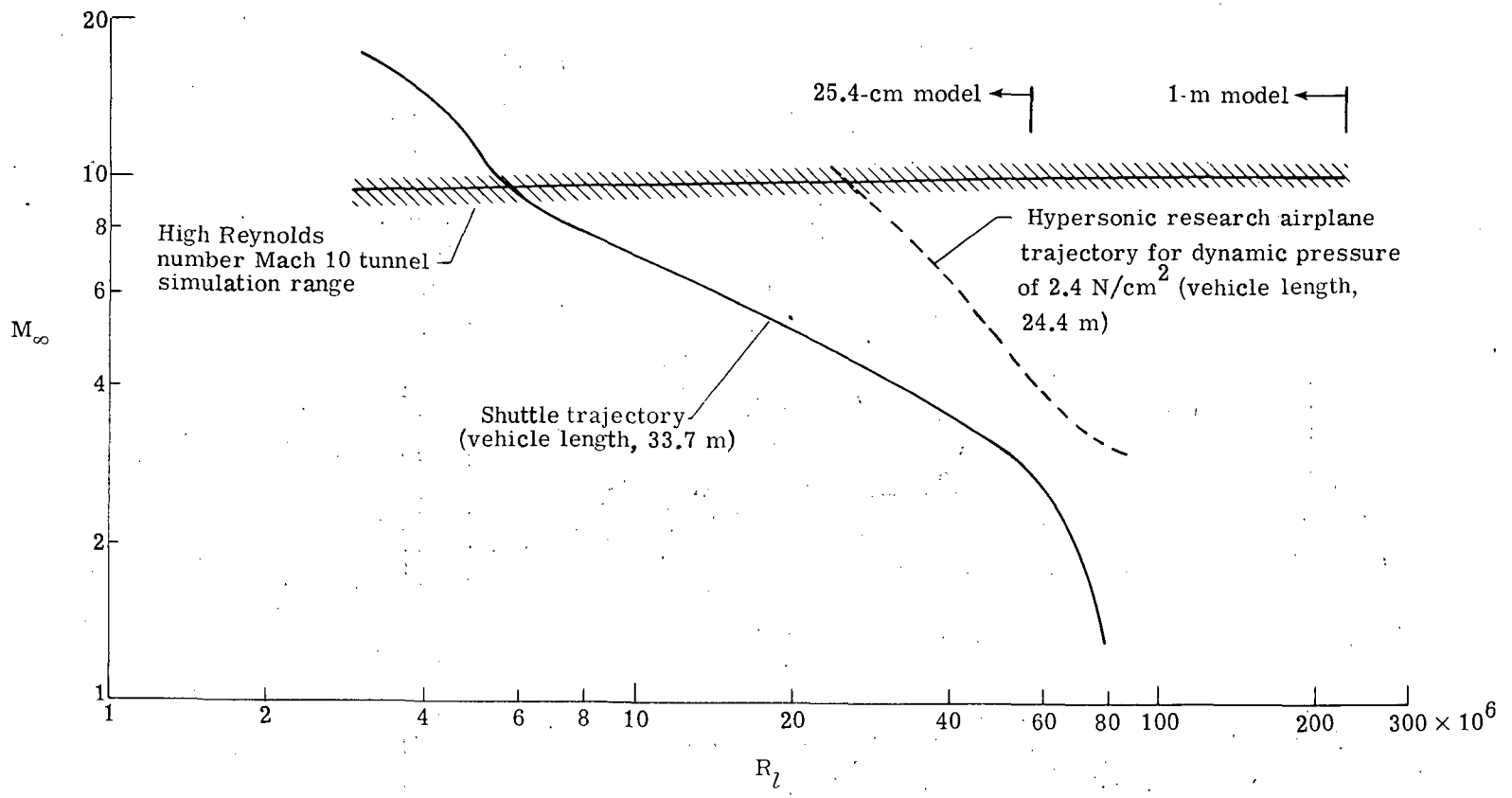

Figure 1.- Mach number-Reynolds number simulation capability of Langley high Reynolds number Mach 10 tunnel.

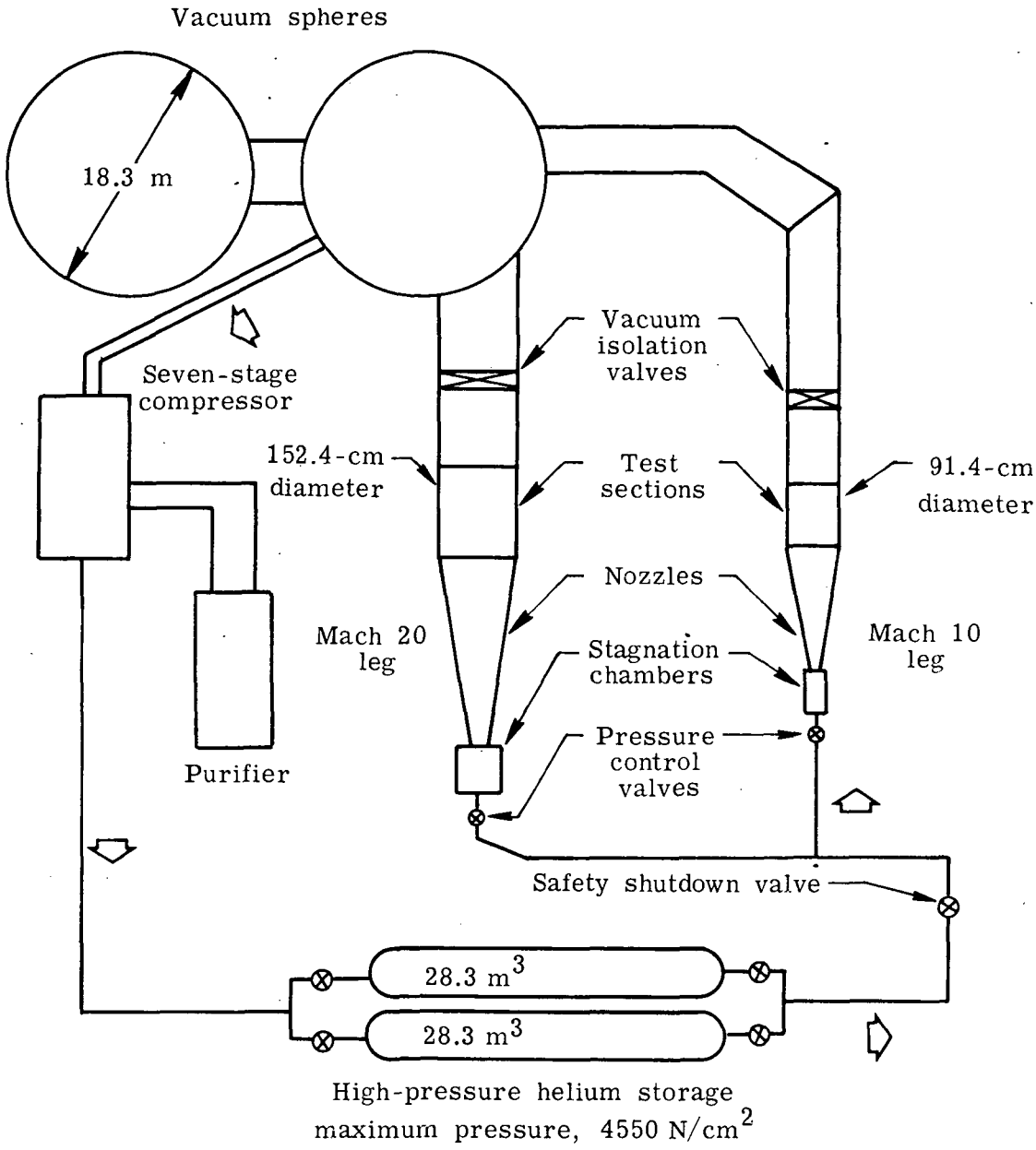

Figure 2.- Schematic diagram of Langley high Reynolds number helium tunnels.

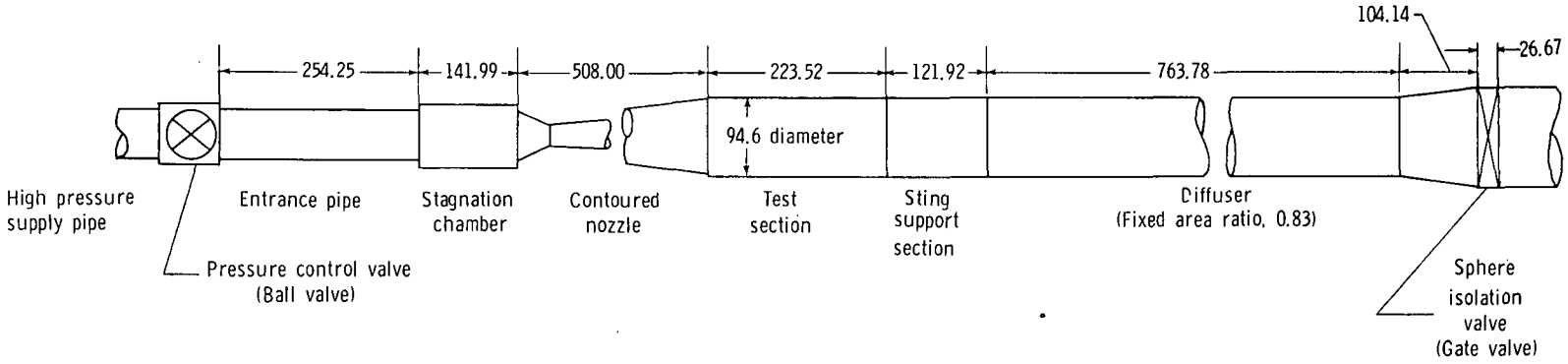

(a) Overall tunnel dimensions are in centimeters.

Figure 3.- Basic dimensions of Mach 10 leg of Langley high Reynolds number helium tunnels.

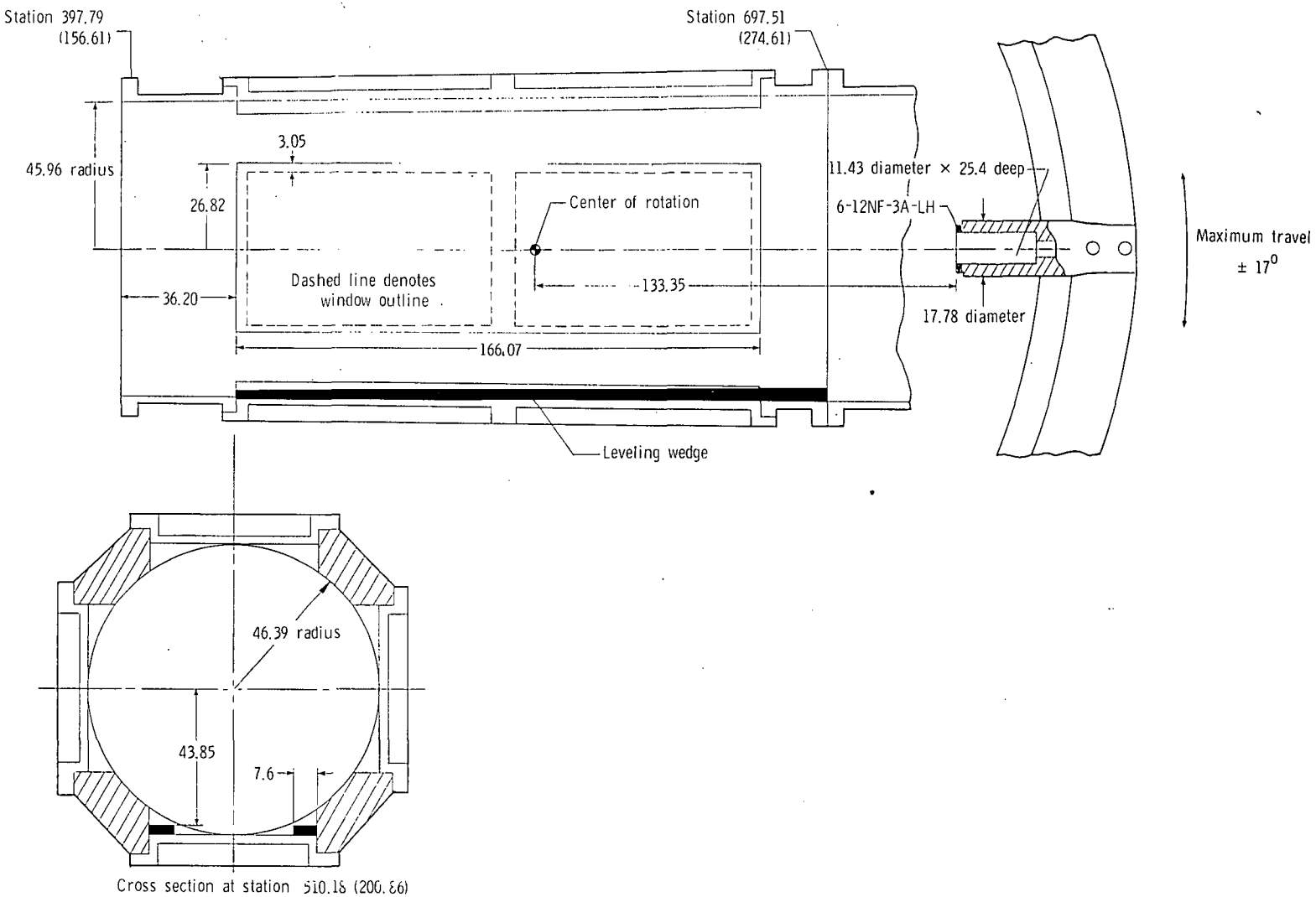

(b) Test-section dimensions and model mounting details. Dimensions are in centimeters. Tunnel stations are cm (in.) from throat.

Figure 3.- Concluded.

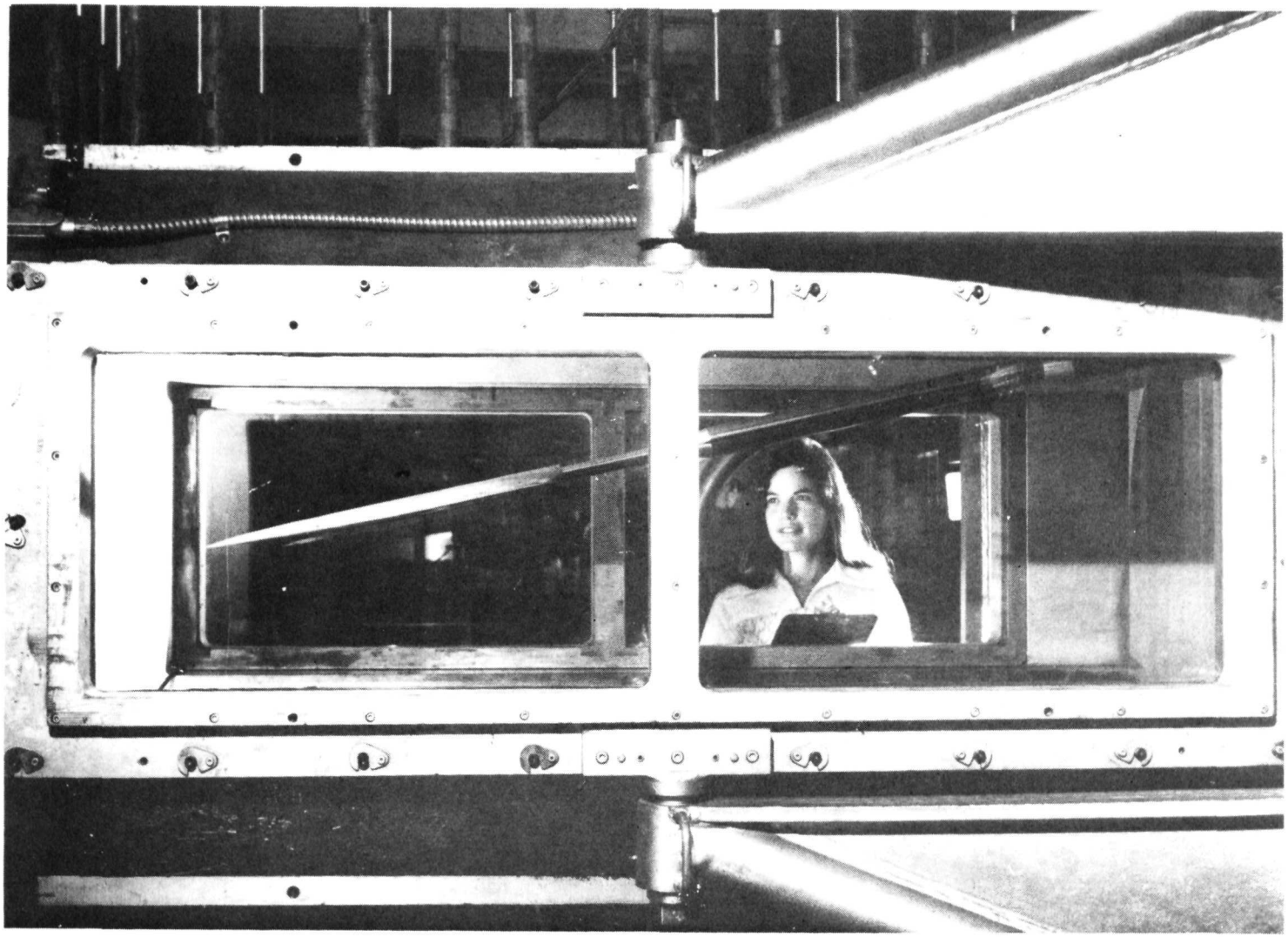

L-73-3806

Figure 4.- Test section of Langley high Reynolds number Mach 10 tunnel. Diameter, 94 cm.

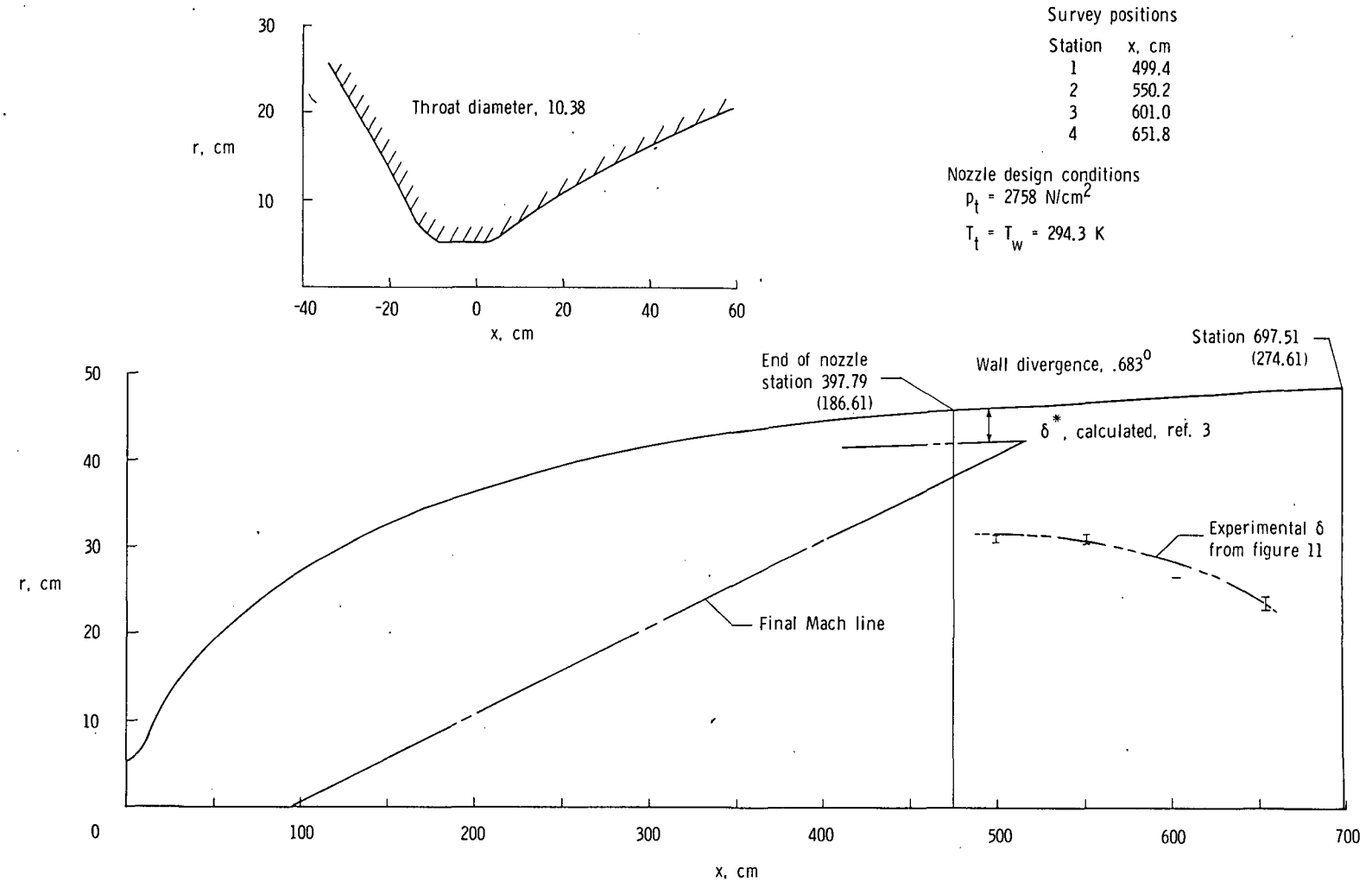

Figure 5.- Nozzle-test-section details.

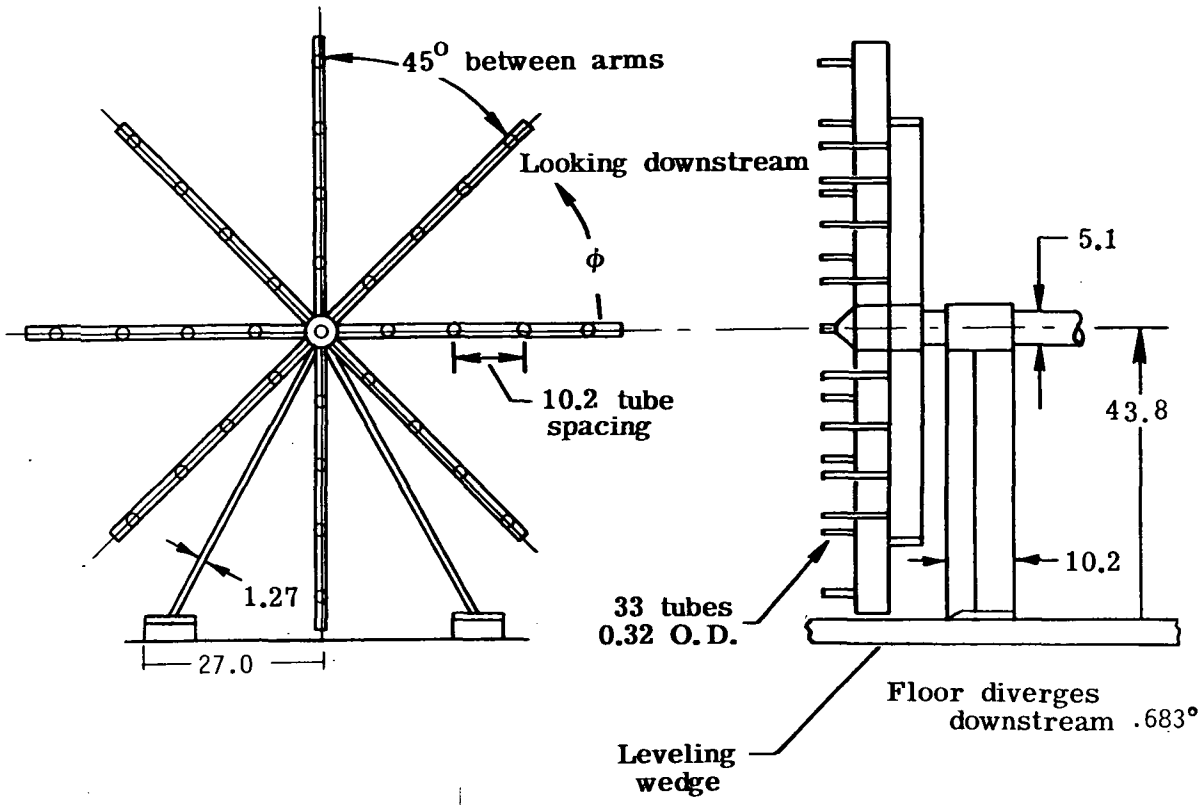

(a) Large rake.

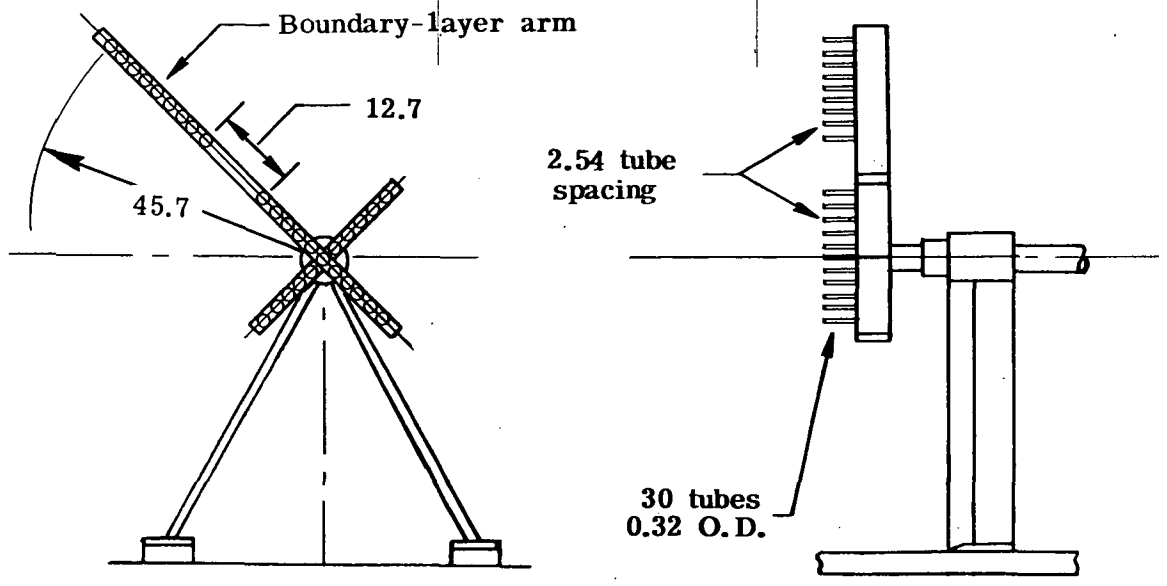

(b) Small rake.

Figure 6.- Pitot rakes. Dimensions are in cm.

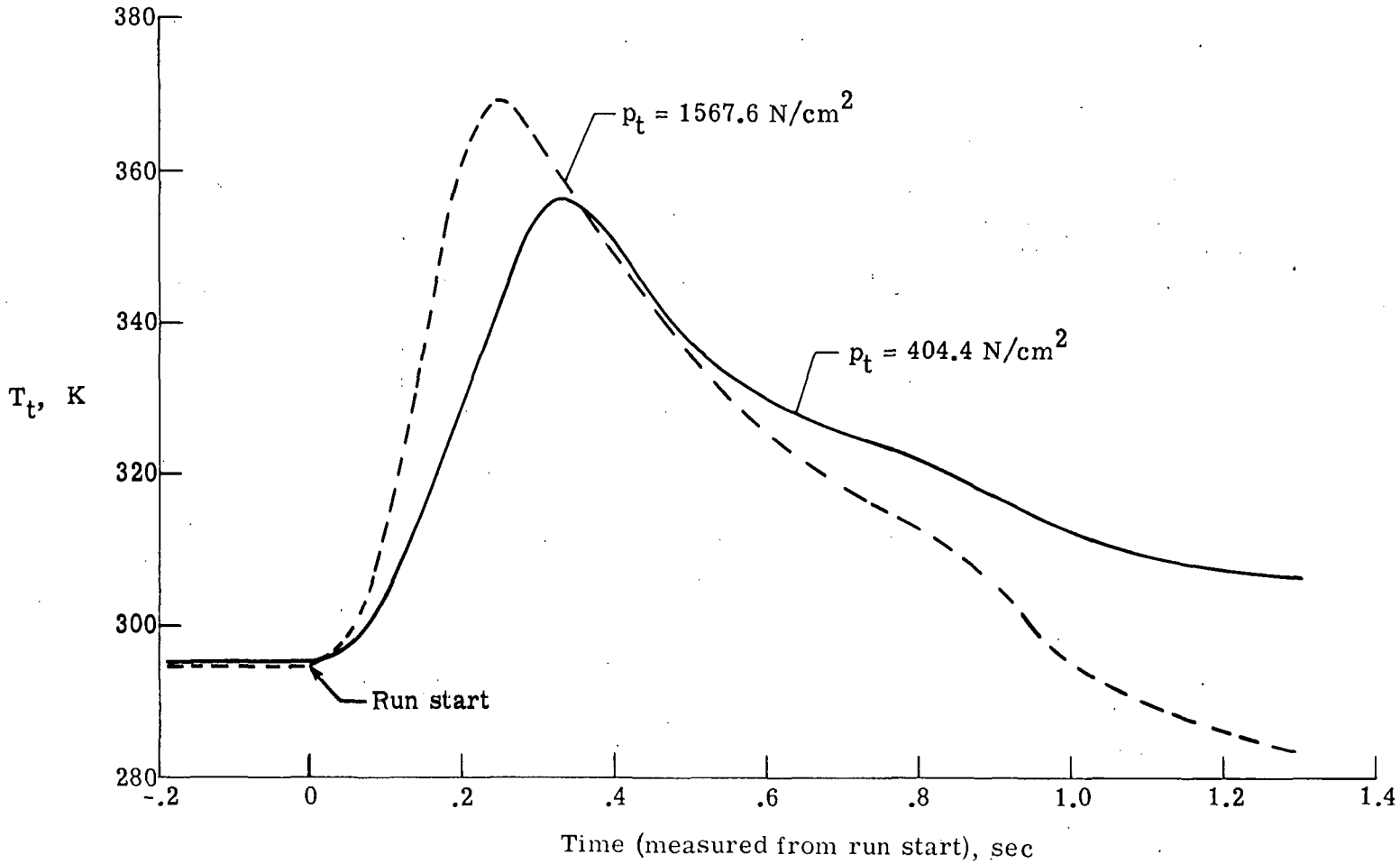

Figure 7.- Total temperature transients during tunnel start.

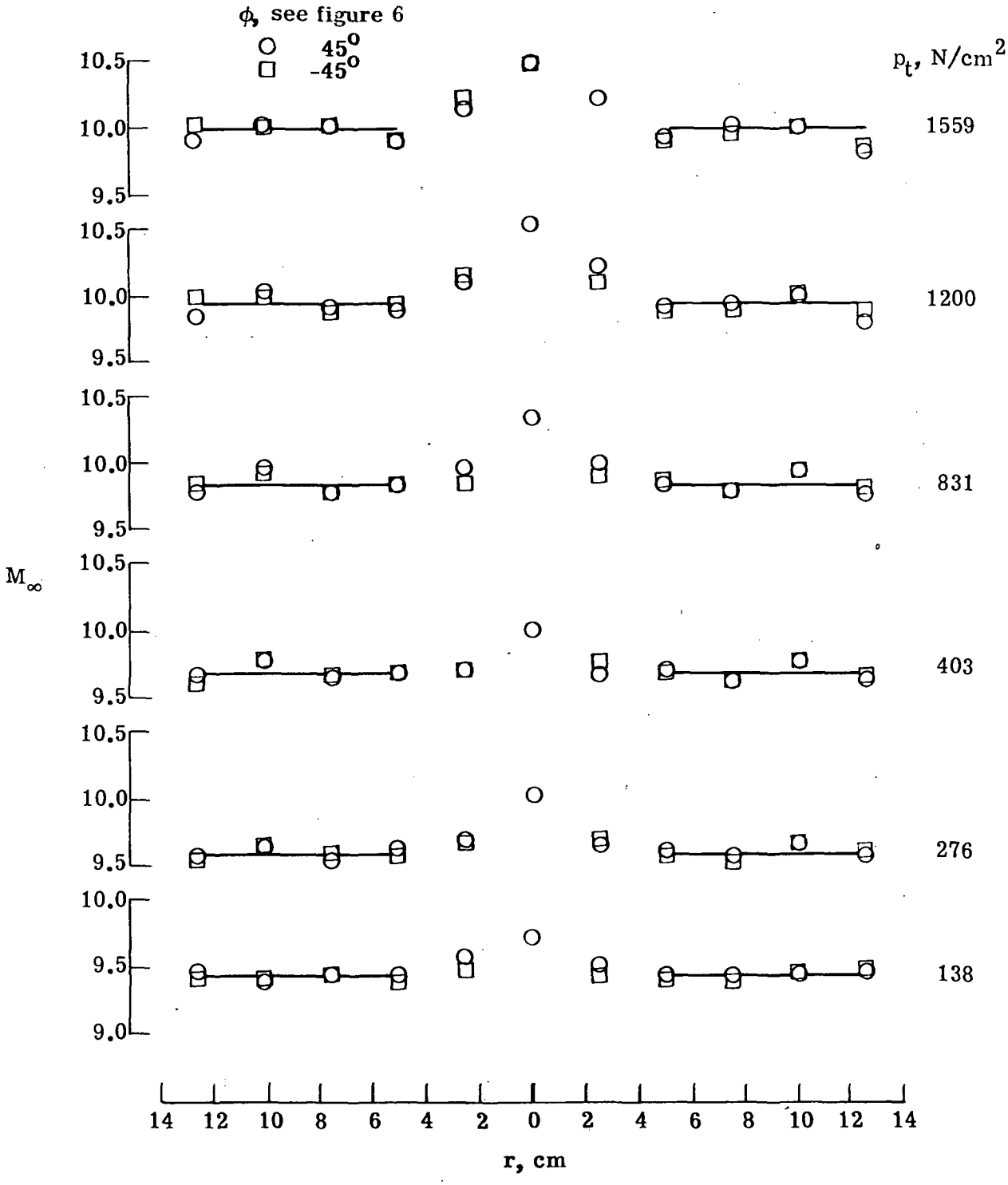

(a) Station 1.

Figure 8.- Mach number distributions using the small rake.

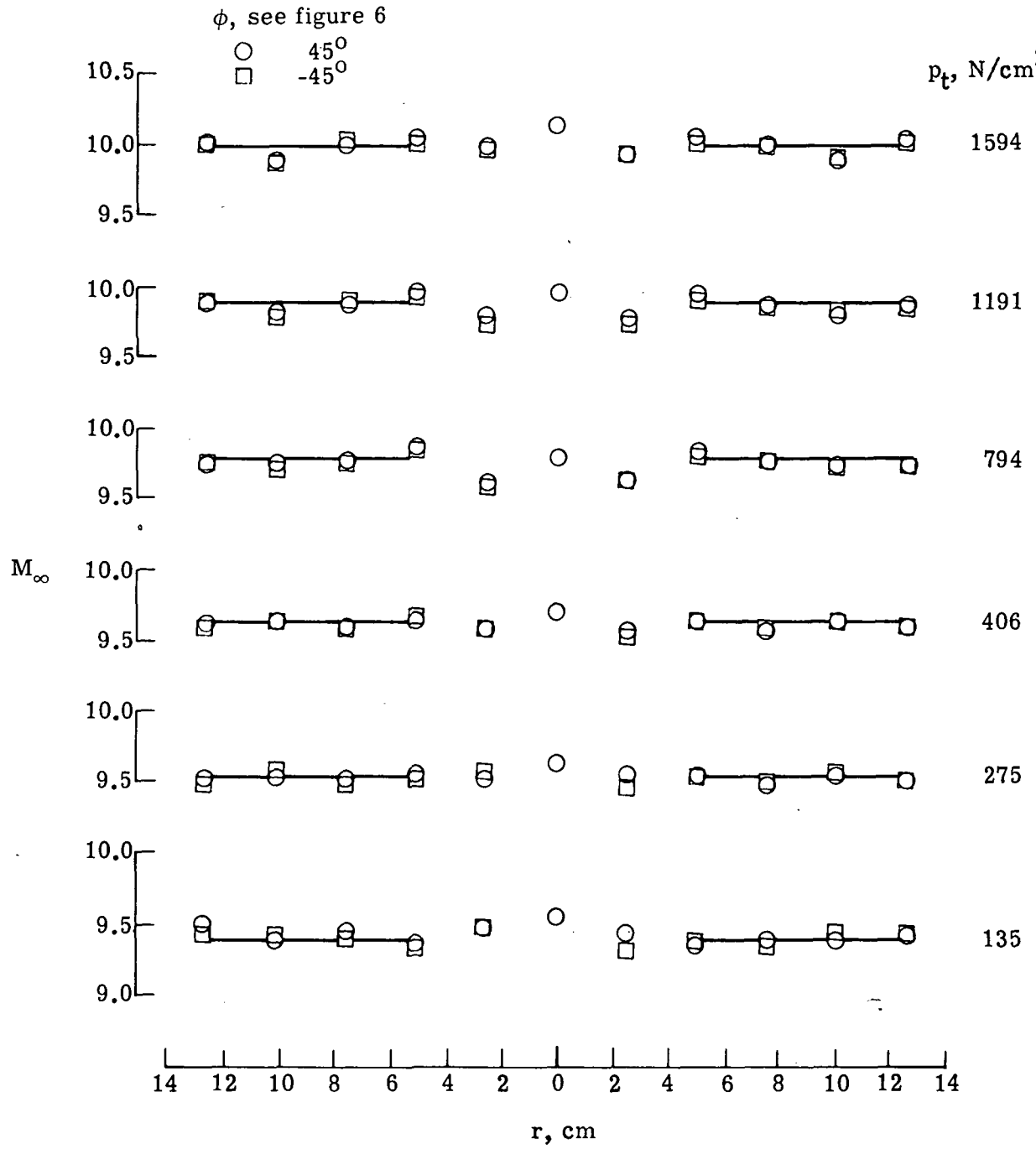

(b) Station 2.

Figure 8.- Continued.

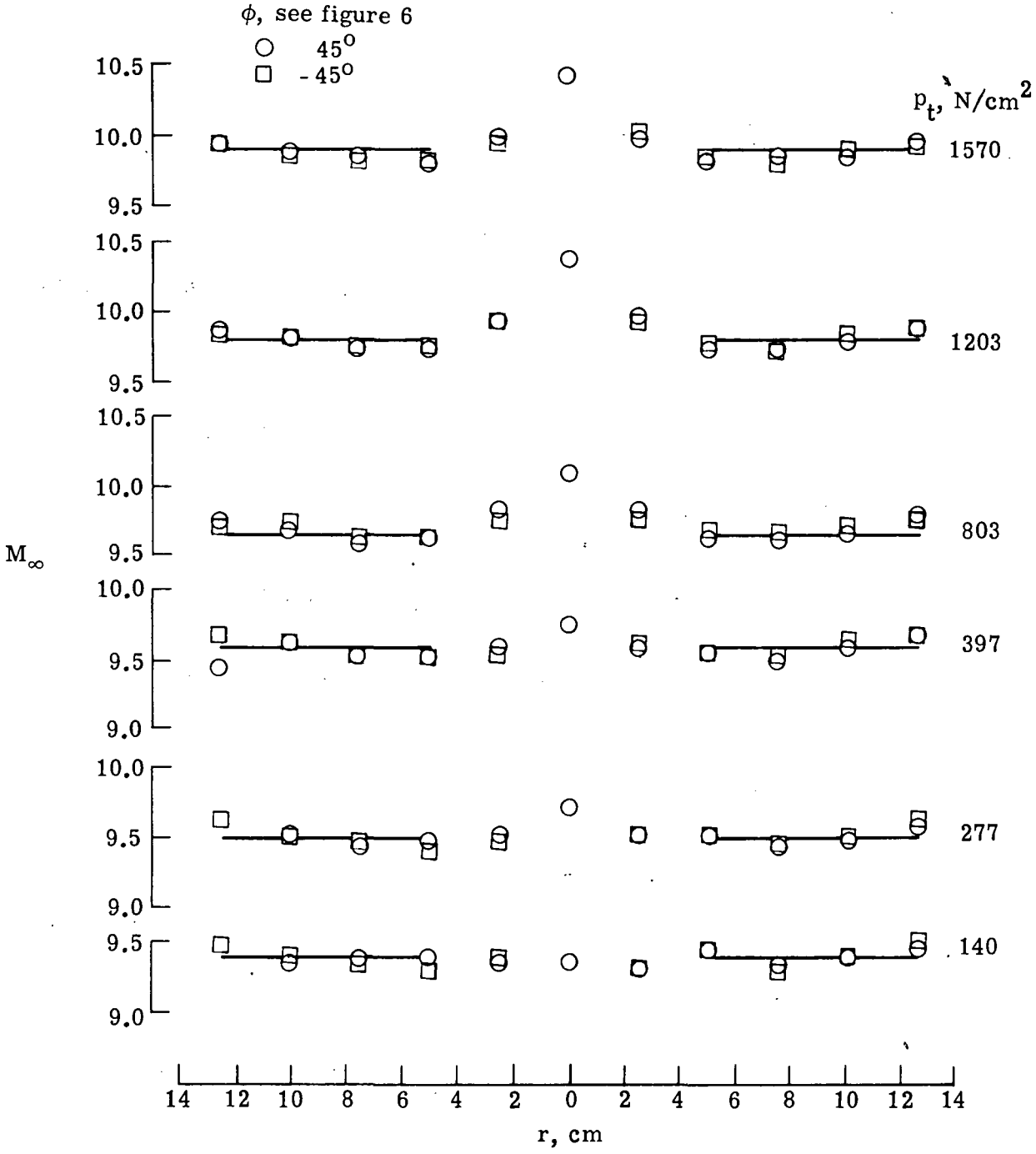

(c) Station 3.

Figure 8.- Continued.

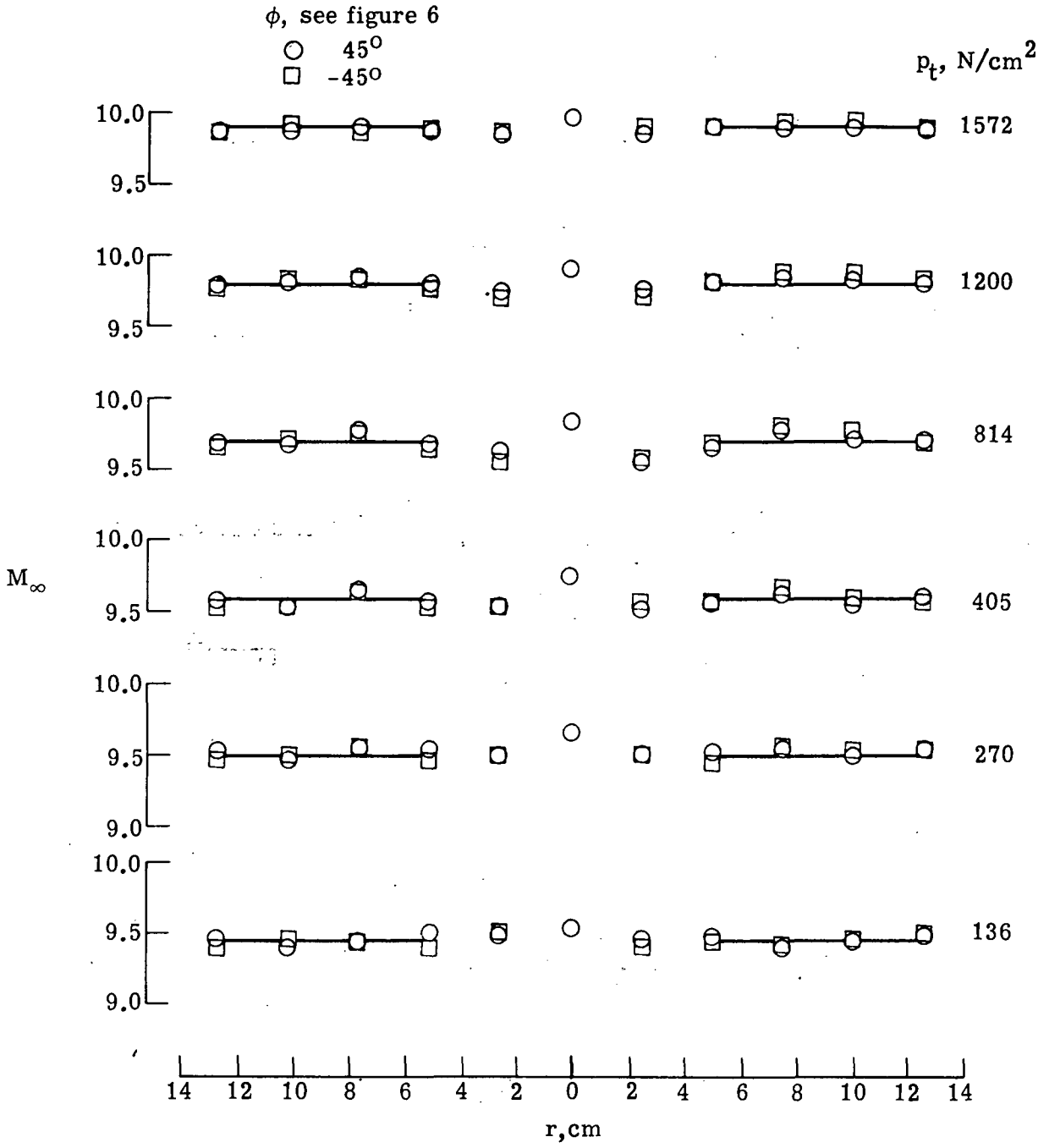

(d) Station 4.

Figure 8.- Concluded.

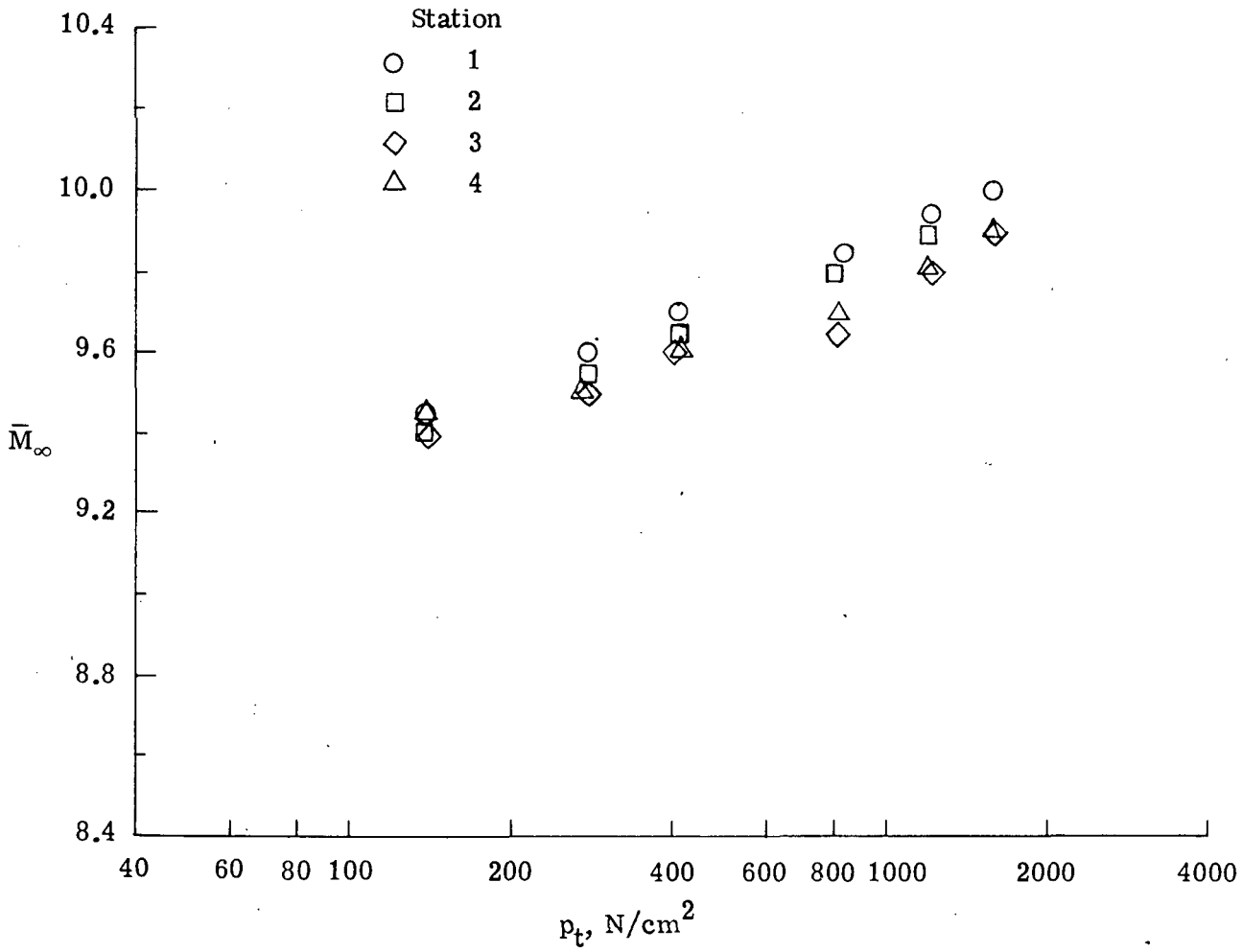

Figure 9.- Variation of average Mach number with tunnel stagnation pressure.

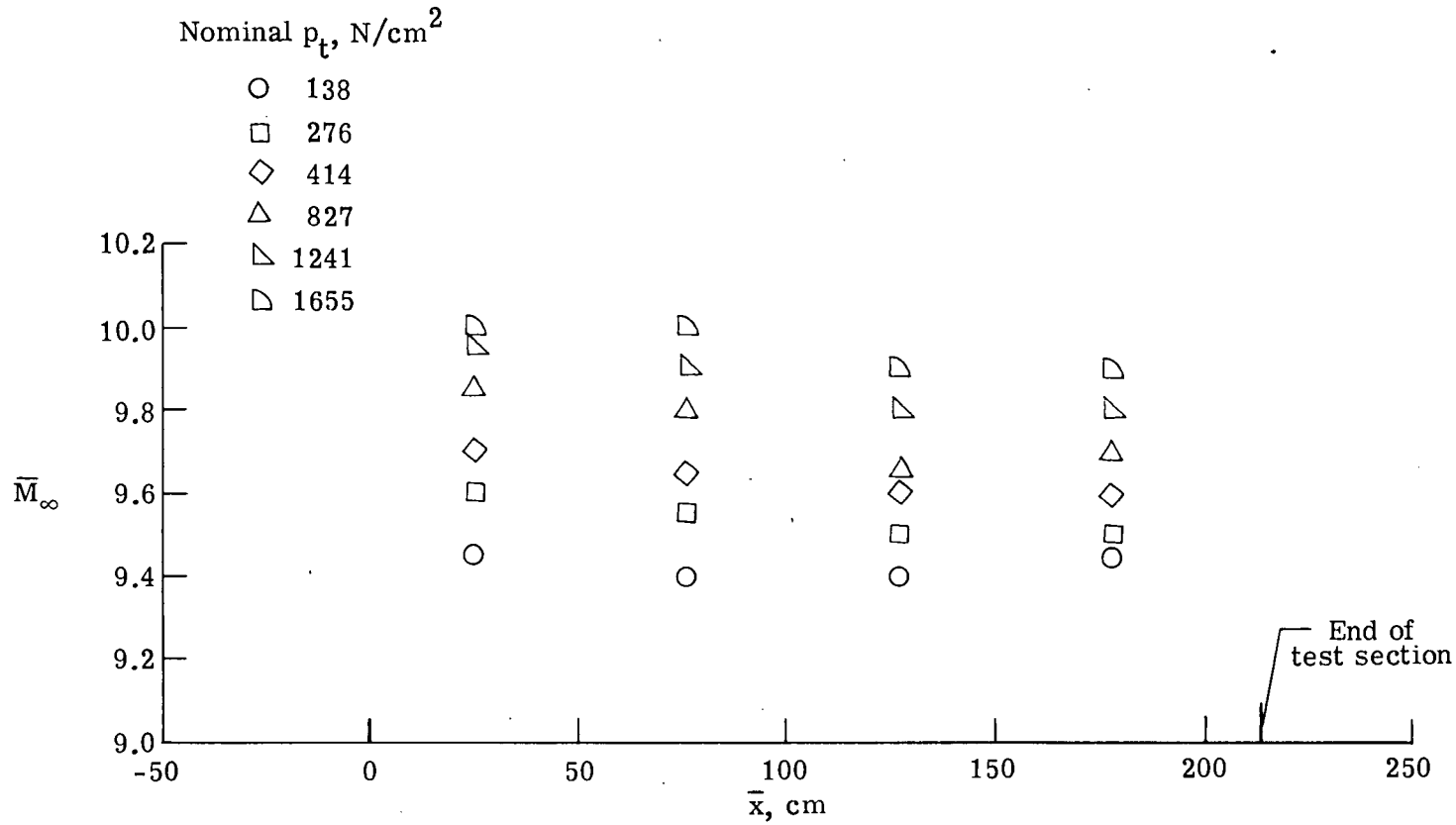

Figure 10.- Variation of average Mach number with axial distance.

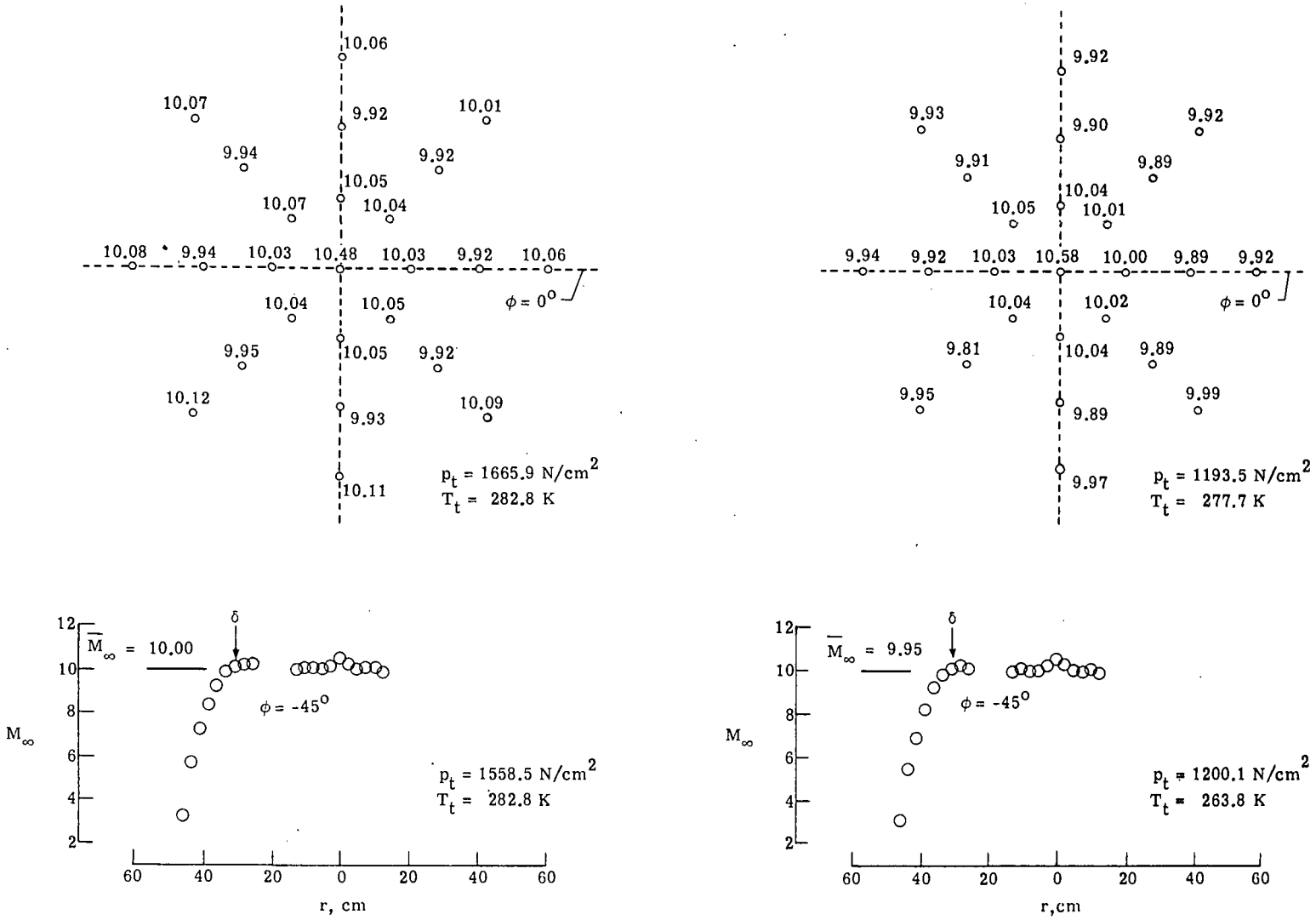

(a) Station 1; p_t = 1600 N/cm^2.

(b) Station 1; p_t = 1200 N/cm^2.

Figure 11.- Mach number distribution in test section.

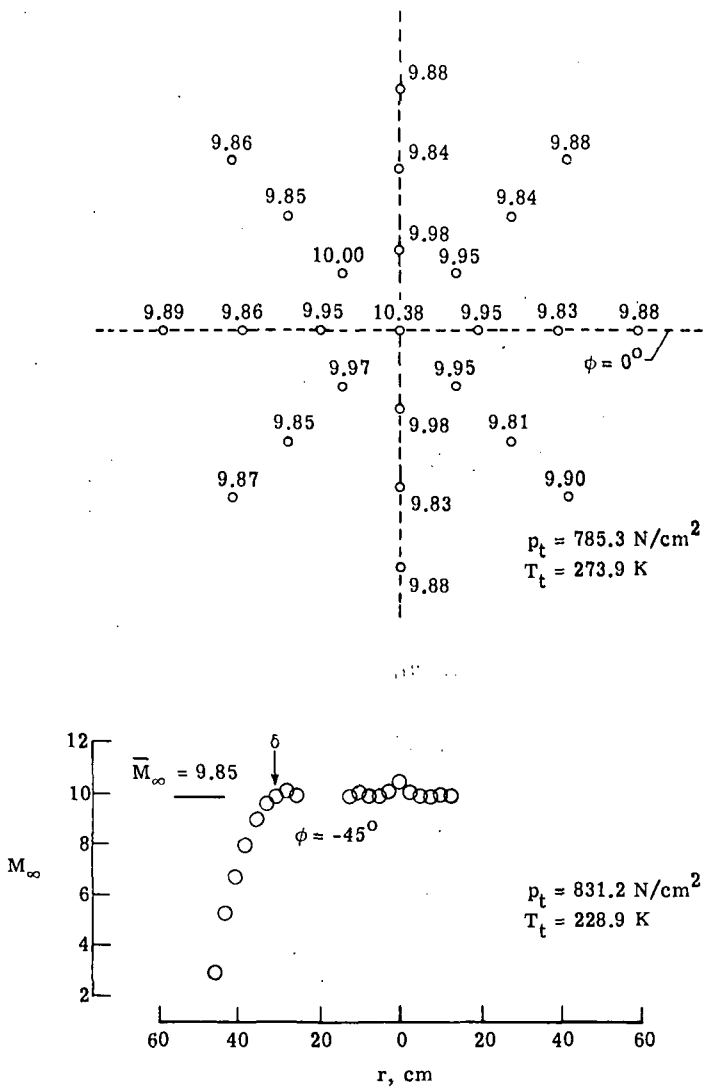

(c) Station 1; p_t = 800 N/cm^2.

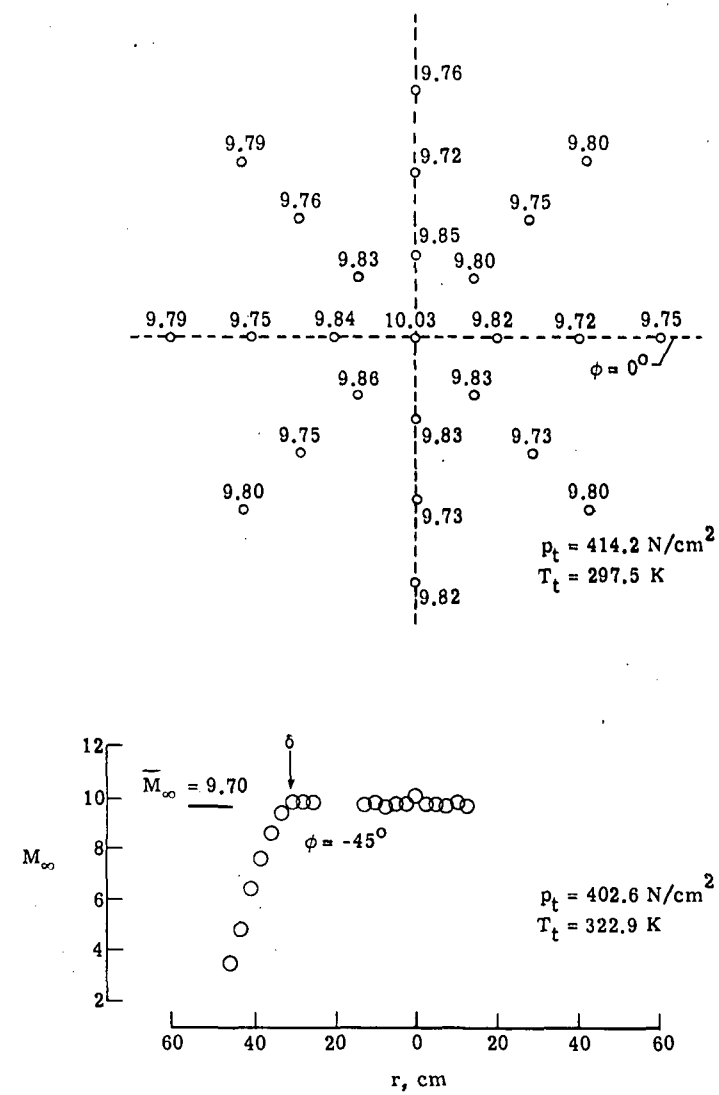

(d) Station 1; p_t = 400 N/cm^2.

Figure 11.- Continued.

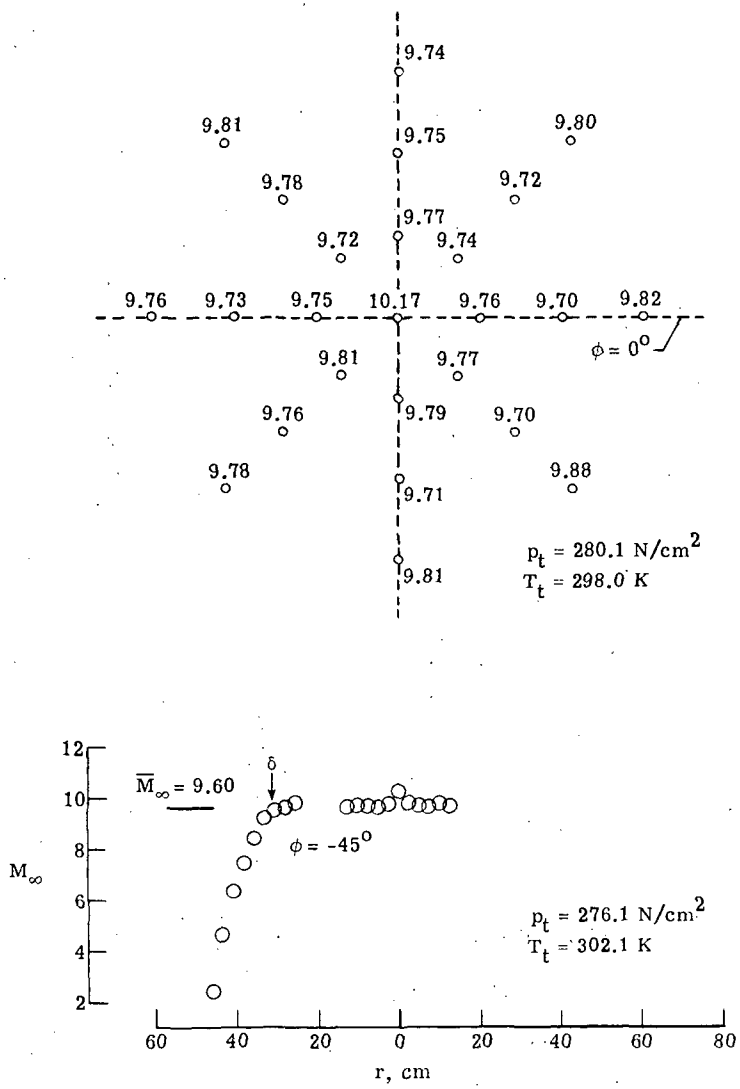

(e) Station 1; p_t = 280 N/cm^2.

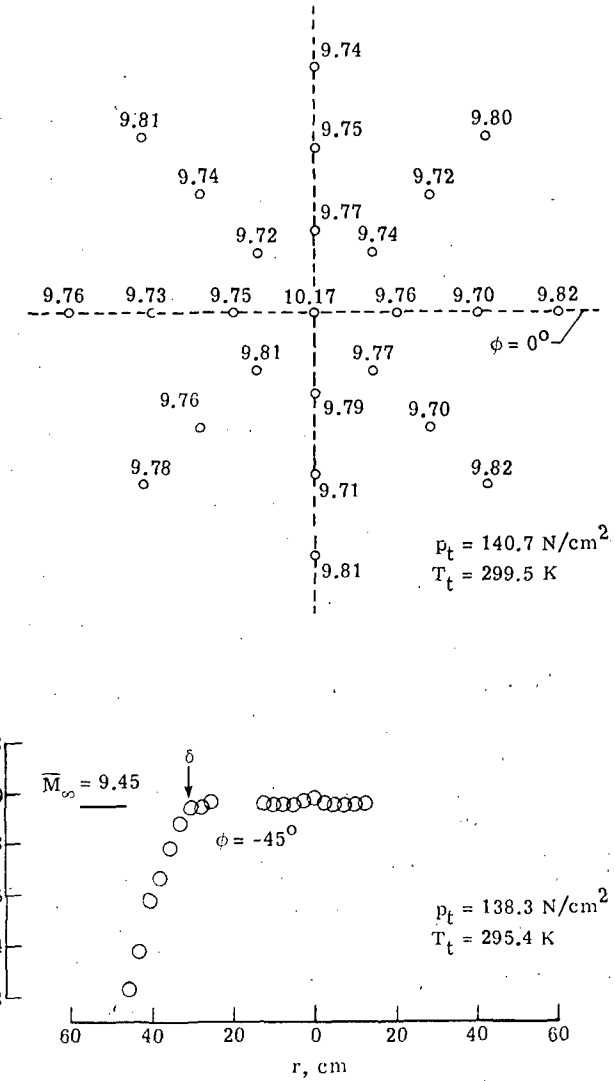

(f) Station 1; p_t = 140 N/cm^2.

Figure 11.- Continued.

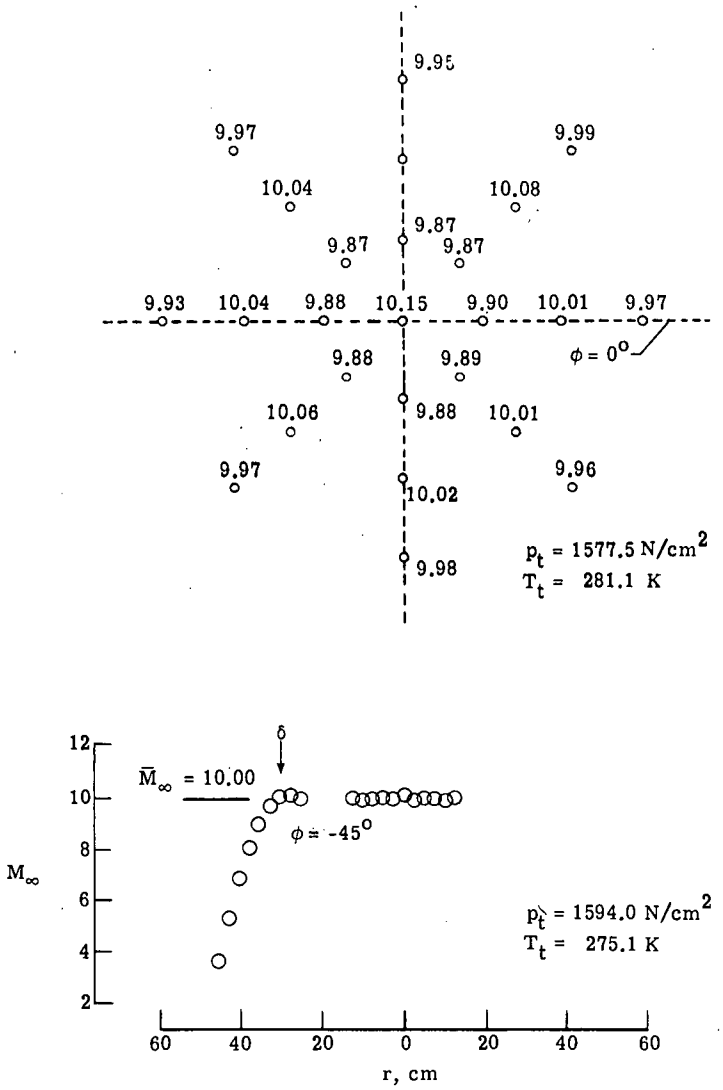

(g) Station 2; p_t = 1600 N/cm^2.

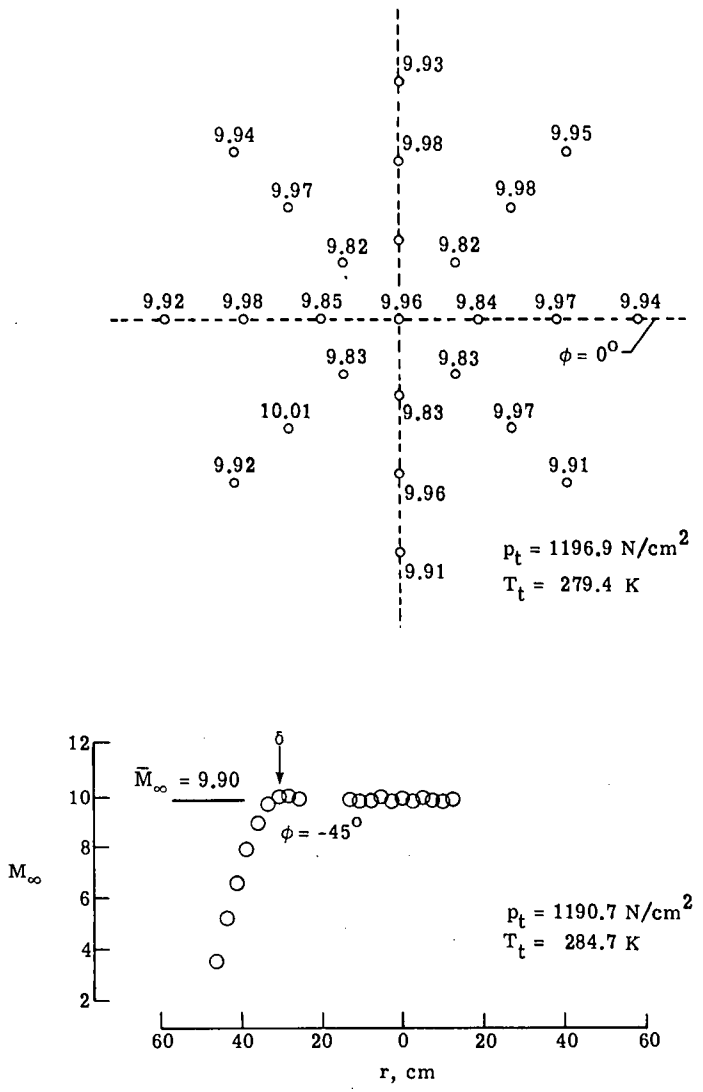

(h) Station 2; p_t = 1200 N/cm^2.

Figure 11.- Continued.

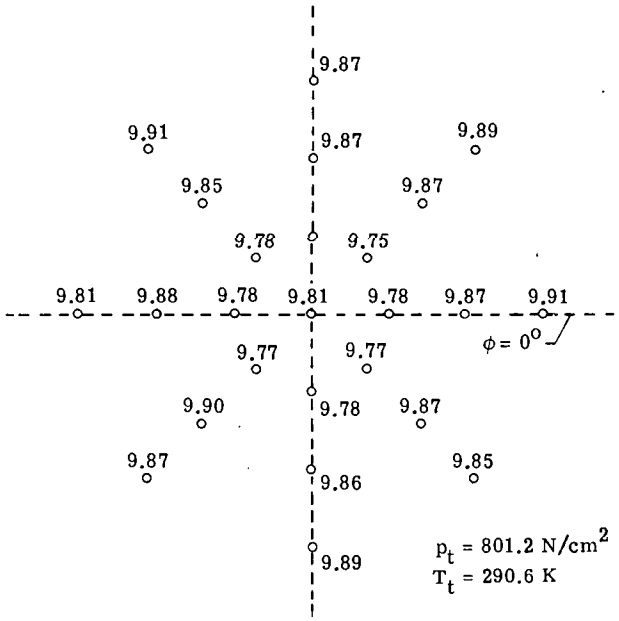

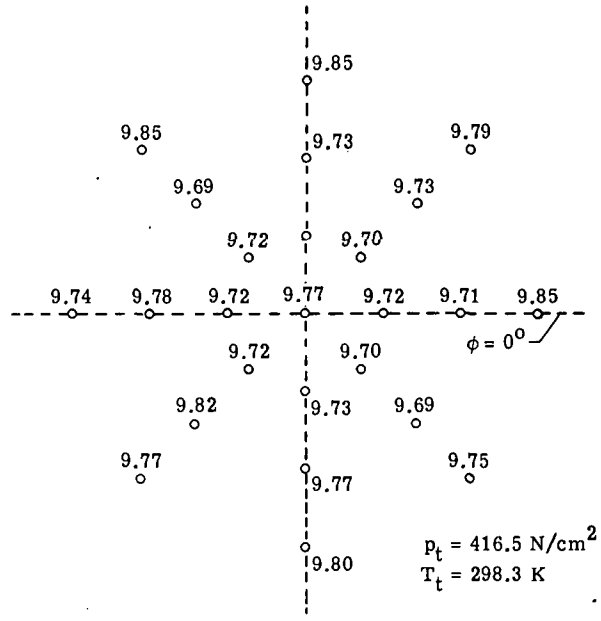

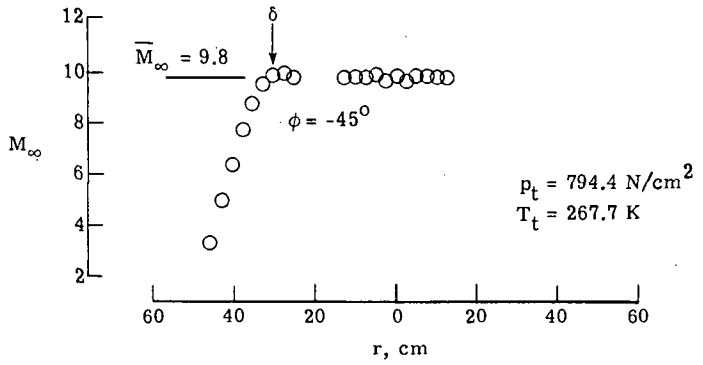

(i) Station 2; p_t = 800 N/cm^2.

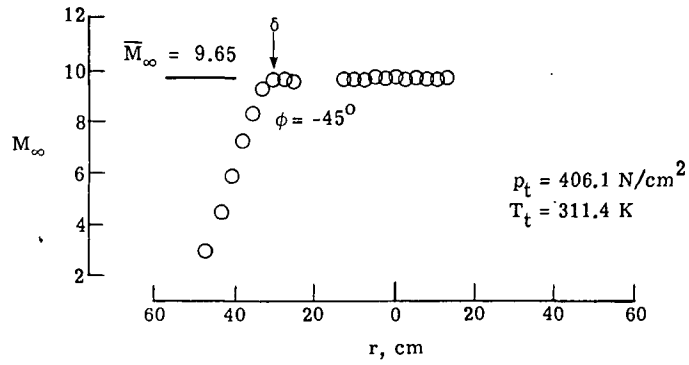

(j) Station 2; p_t = 400 N/cm^2.

Figure 11.- Continued.

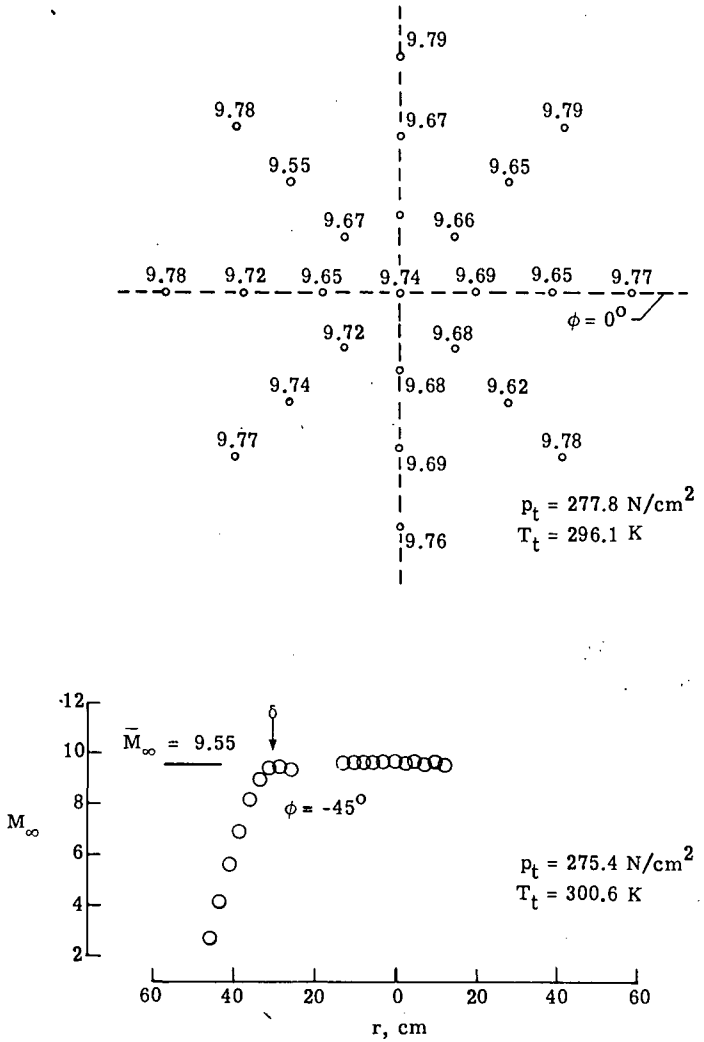

(k) Station 2; $p_t = 280$ N/cm^2.

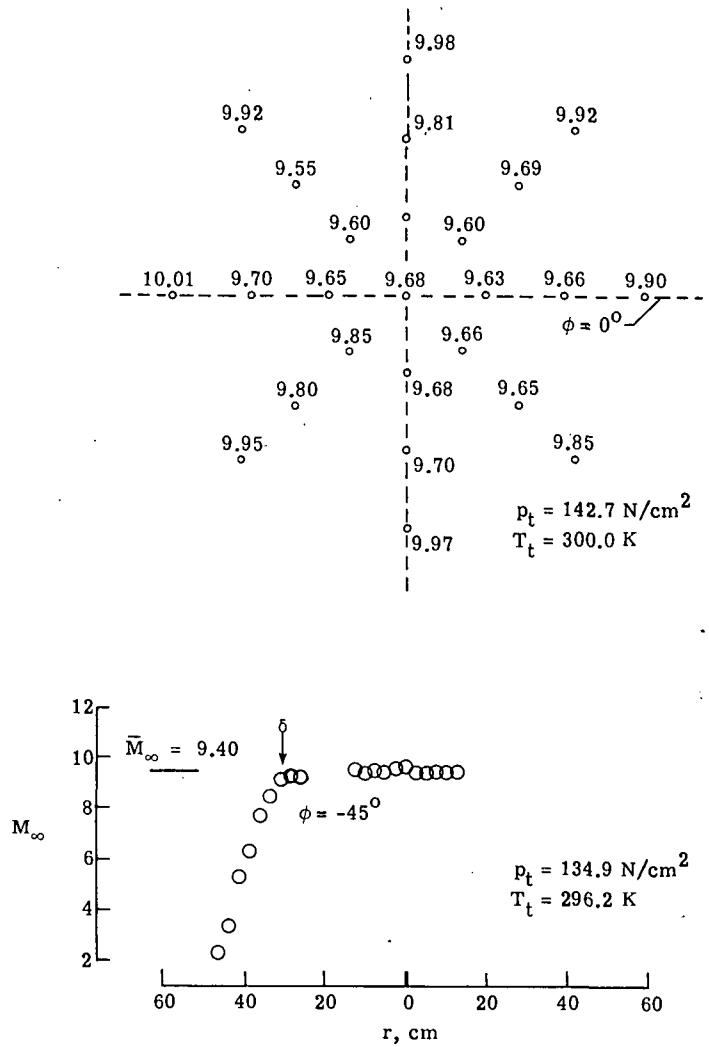

(l) Station 2; $p_t = 140$ N/cm^2.

Figure 11.- Continued.

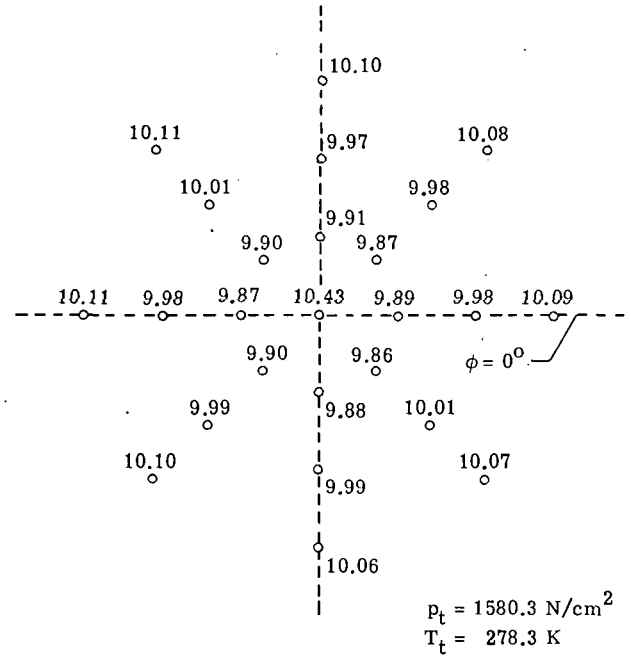

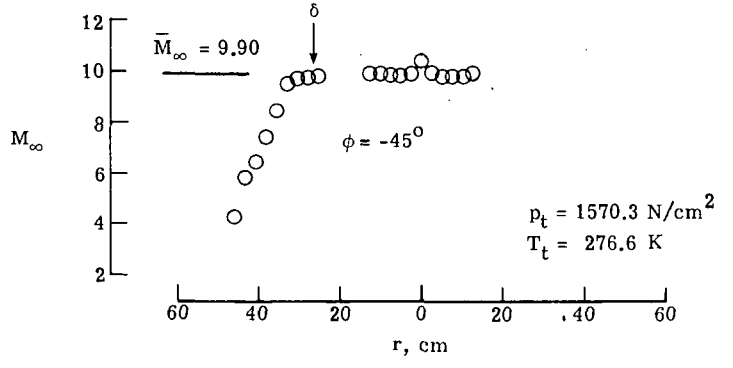

(m) Station 3; p_t = 1600 N/cm^2.

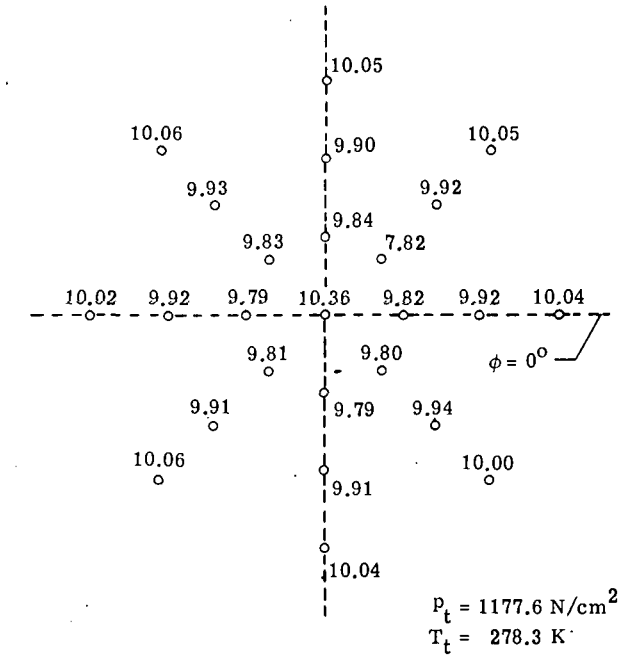

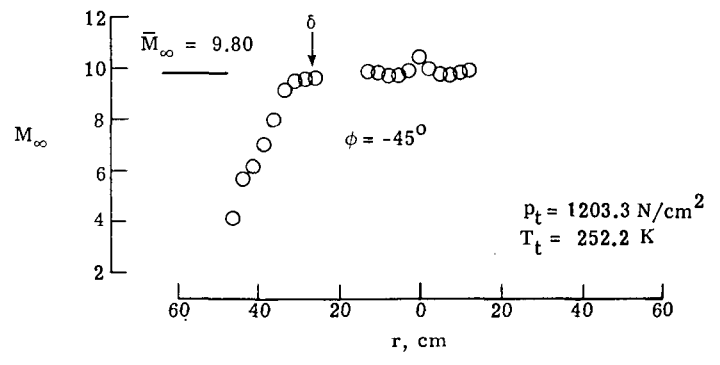

(n) Station 3; p_t = 1200 N/cm^2.

Figure 11.- Continued.

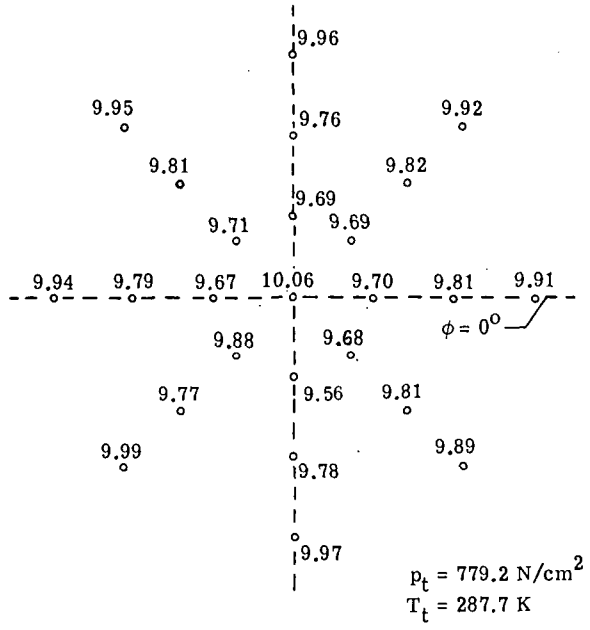

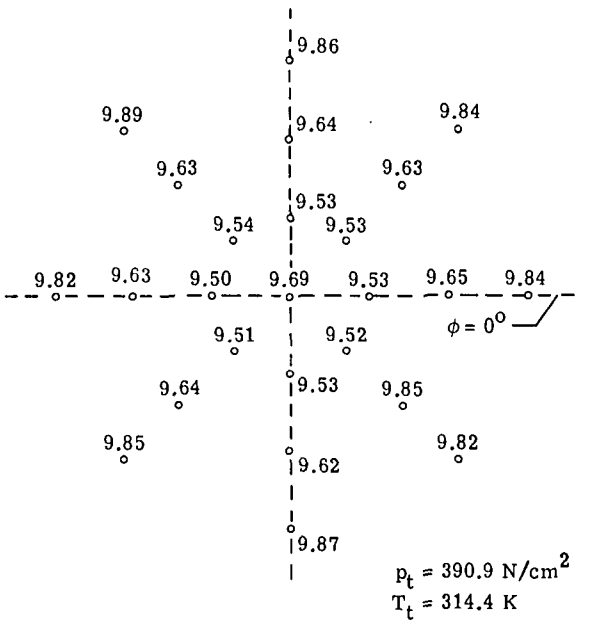

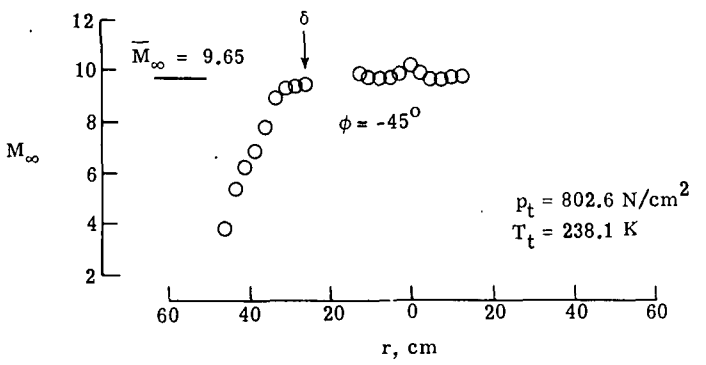

(o) Station 3; p_t = 800 N/cm^2.

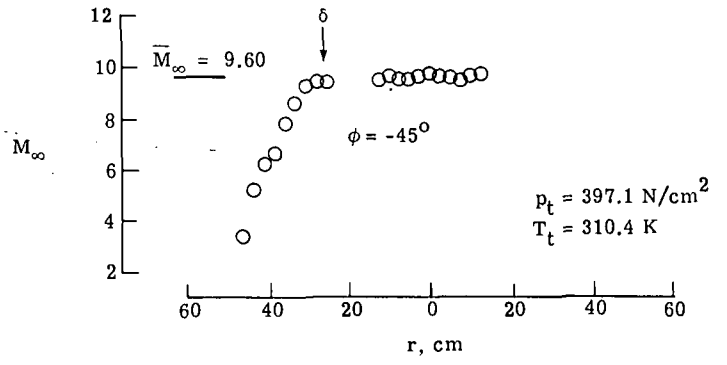

(p) Station 3; p_t = 400 N/cm^2.

Figure 11.- Continued.

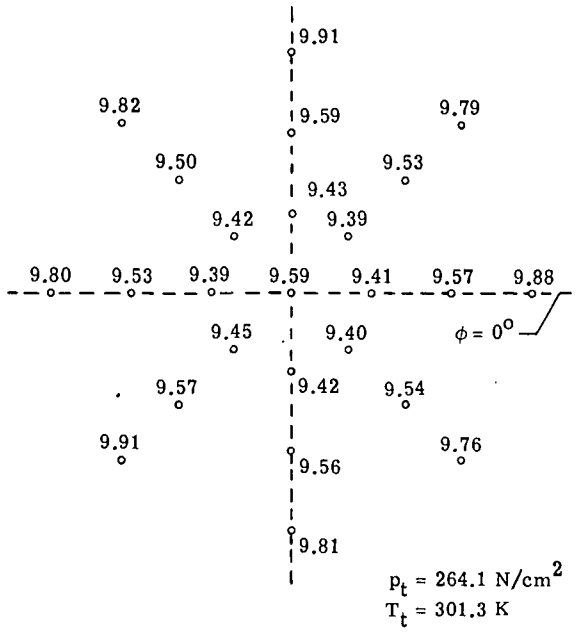

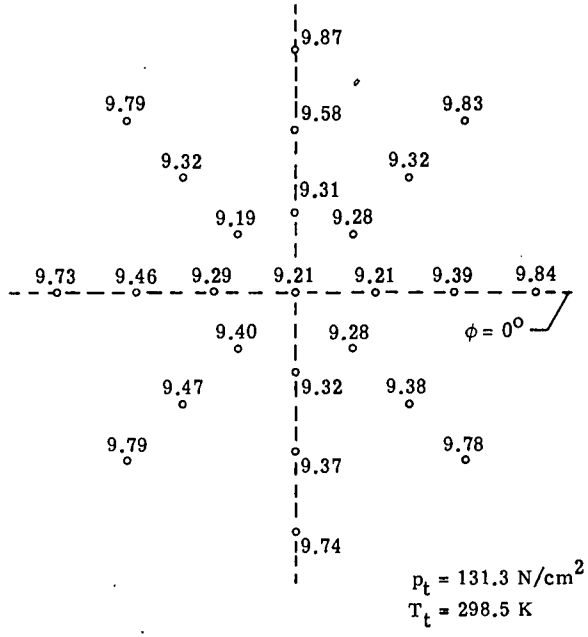

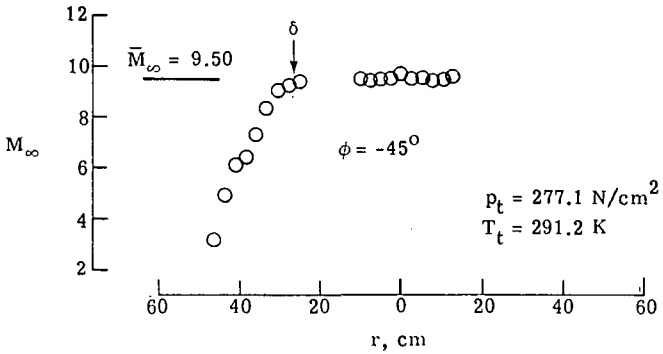

(q) Station 3; p_t = 280 N/cm^2.

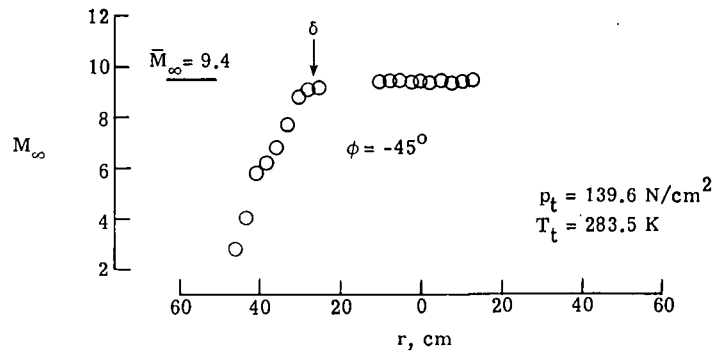

(r) Station 3; p_t = 140 N/cm^2.

Figure 11.- Continued.

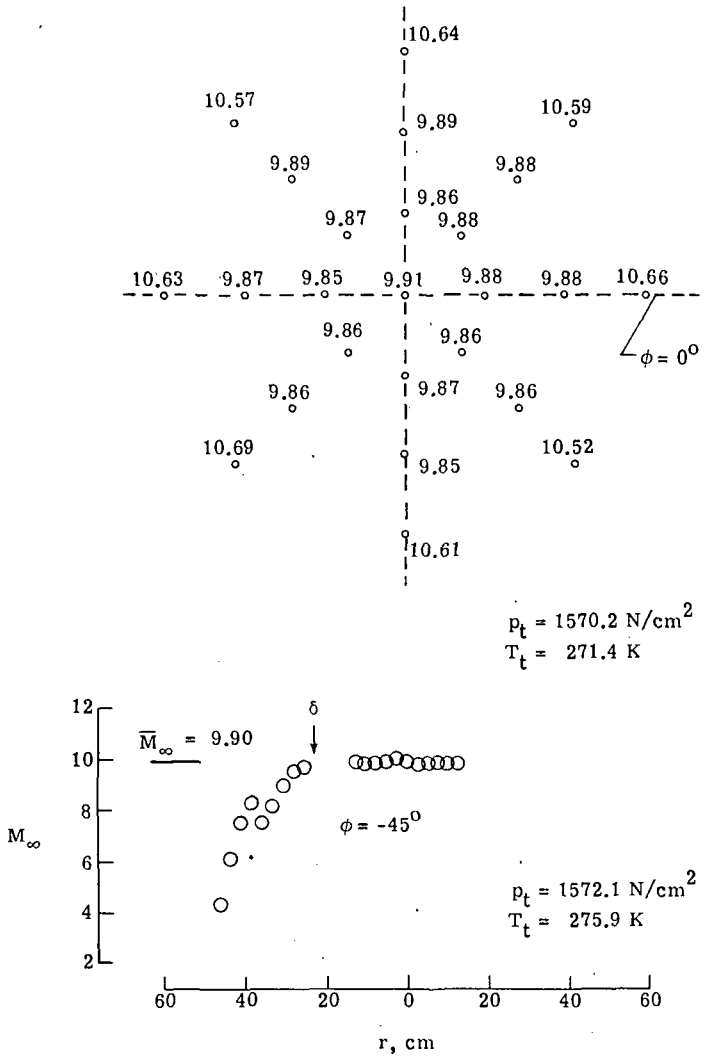

(s) Station 4; p_t = 1600 N/cm^2.

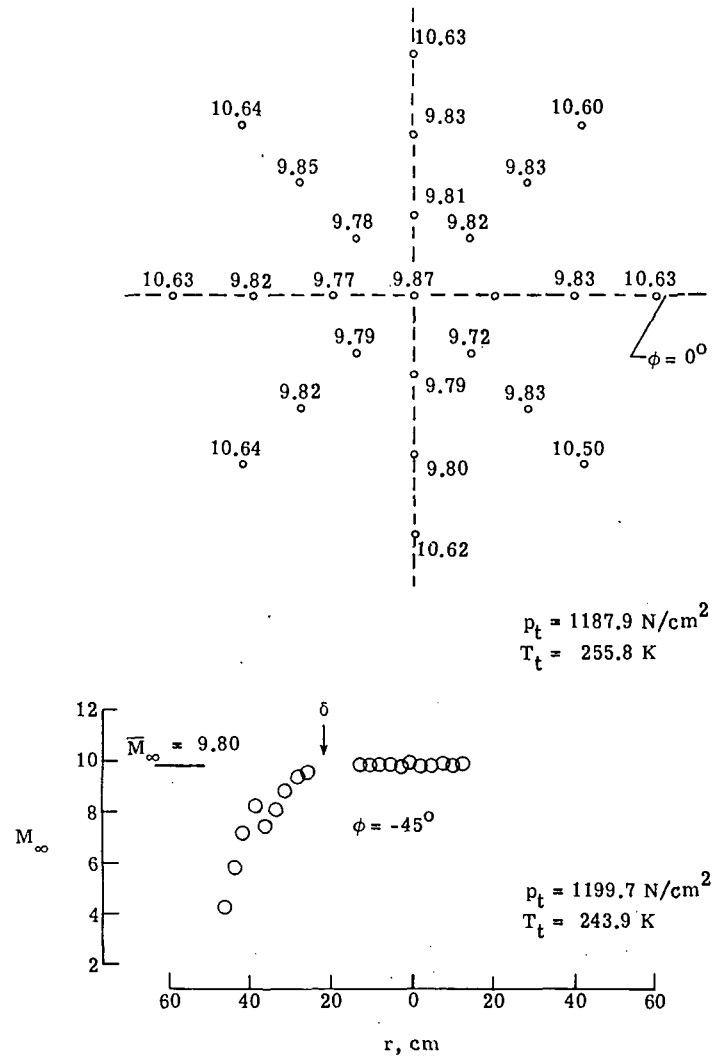

(t) Station 4; p_t = 1200 N/cm^2.

Figure 11.- Continued.

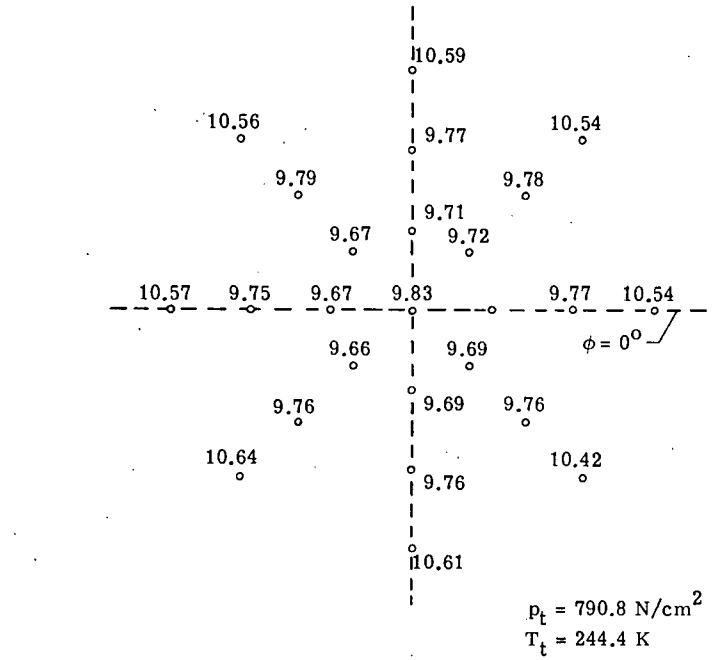

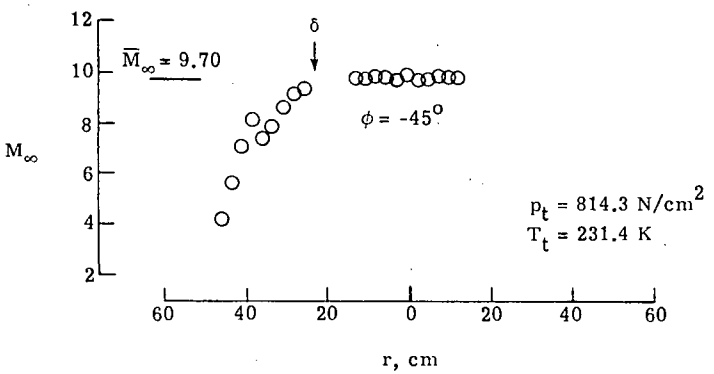

(u) Station 4; p_t = 800 N/cm^2.

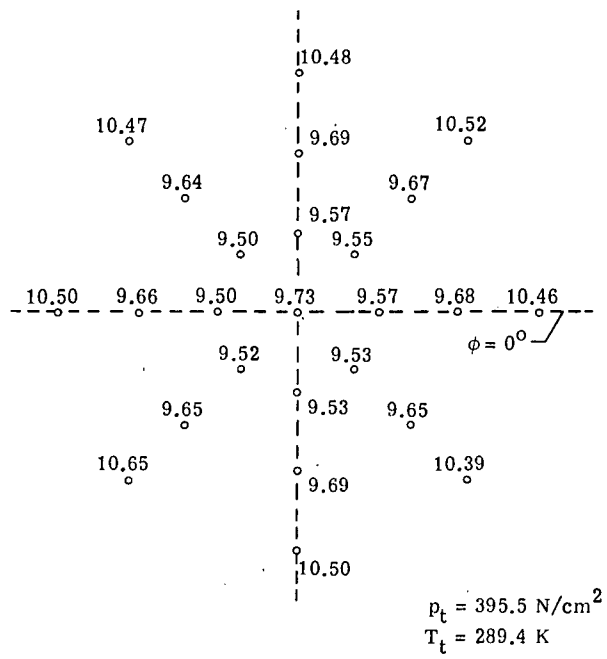

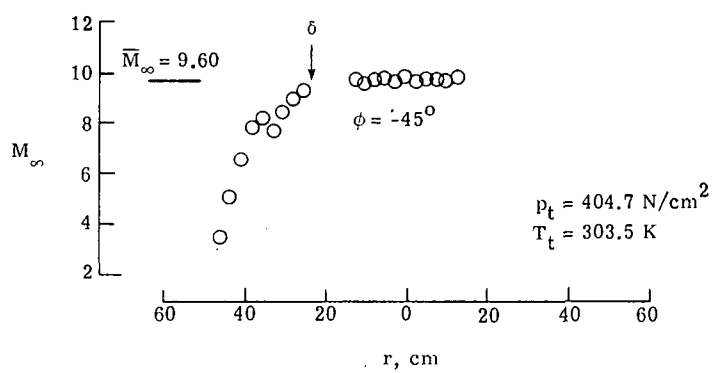

(v) Station 4; p_t = 400 N/cm^2.

Figure 11.- Continued.

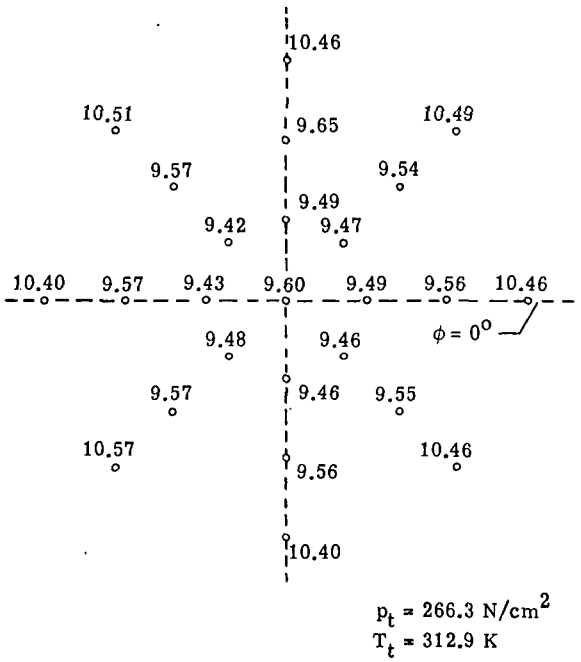

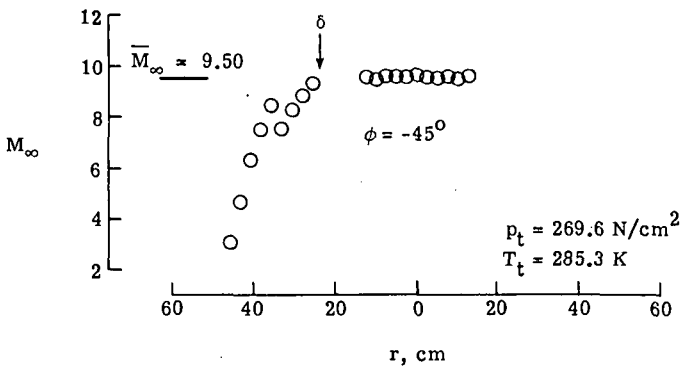

(w) Station 4; p_t = 280 N/cm^2.

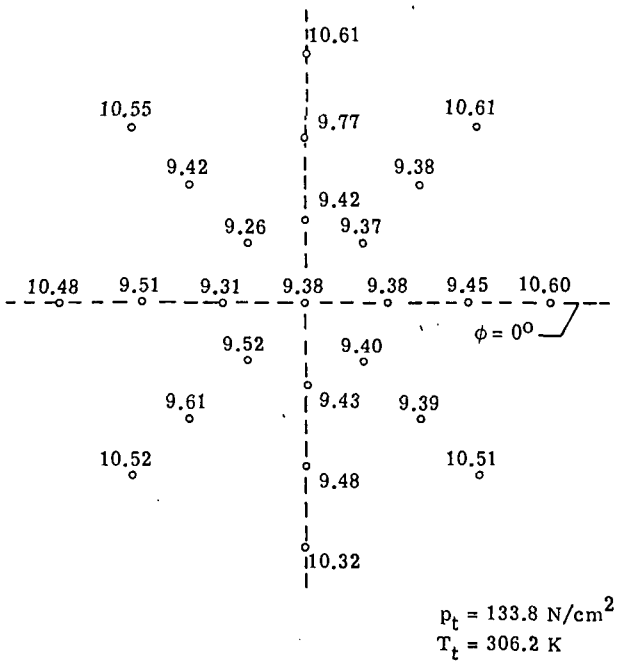

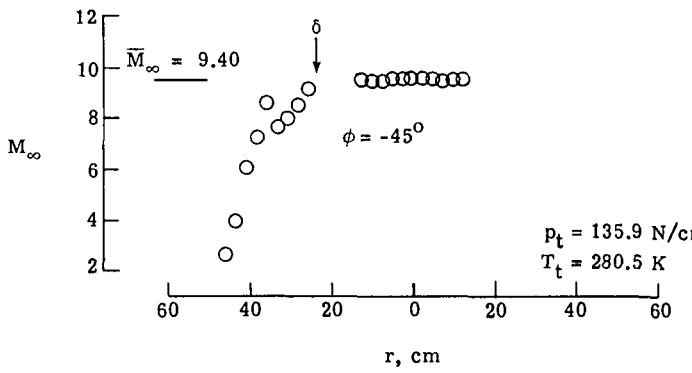

(x) Station 4; p_t = 140 N/cm^2.

Figure 11.- Concluded.

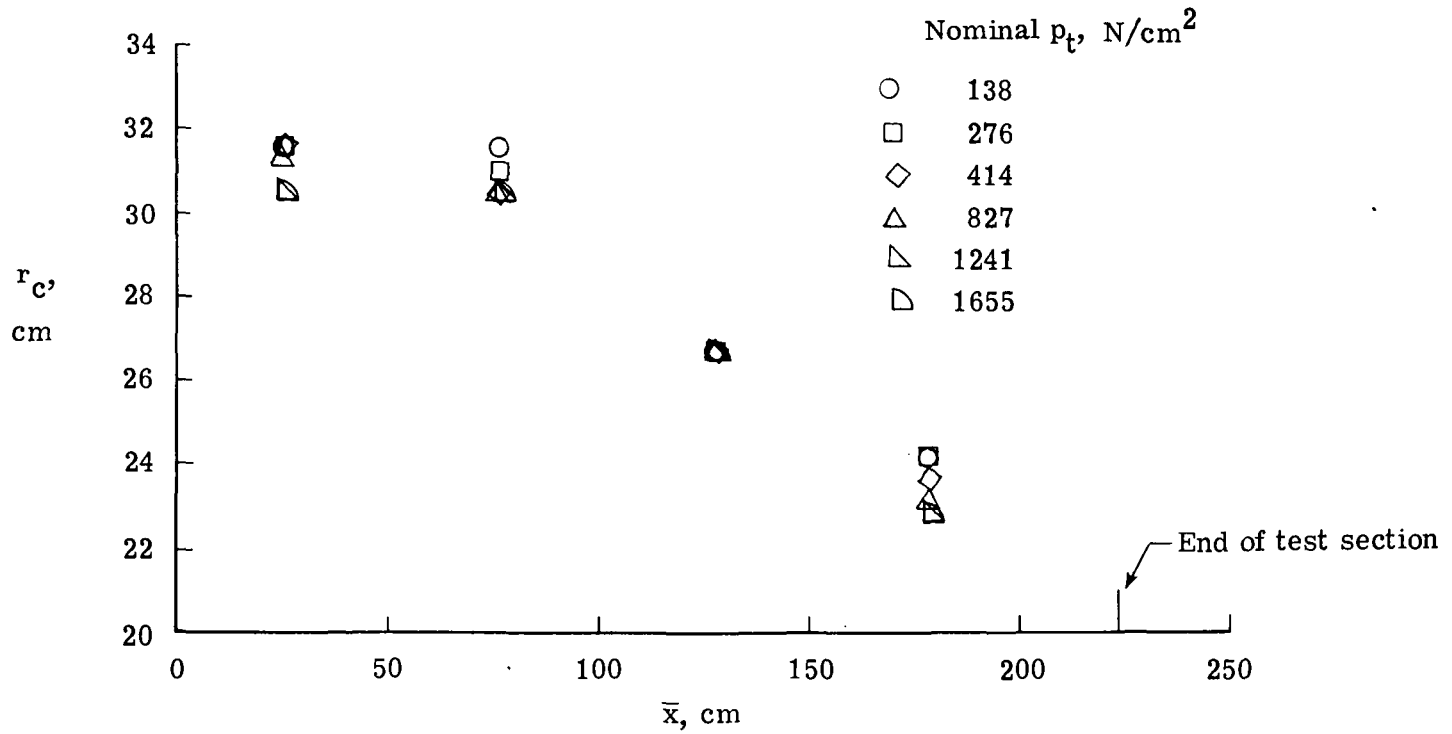

Figure 12.- Variation of inviscid core radius with test-section length.

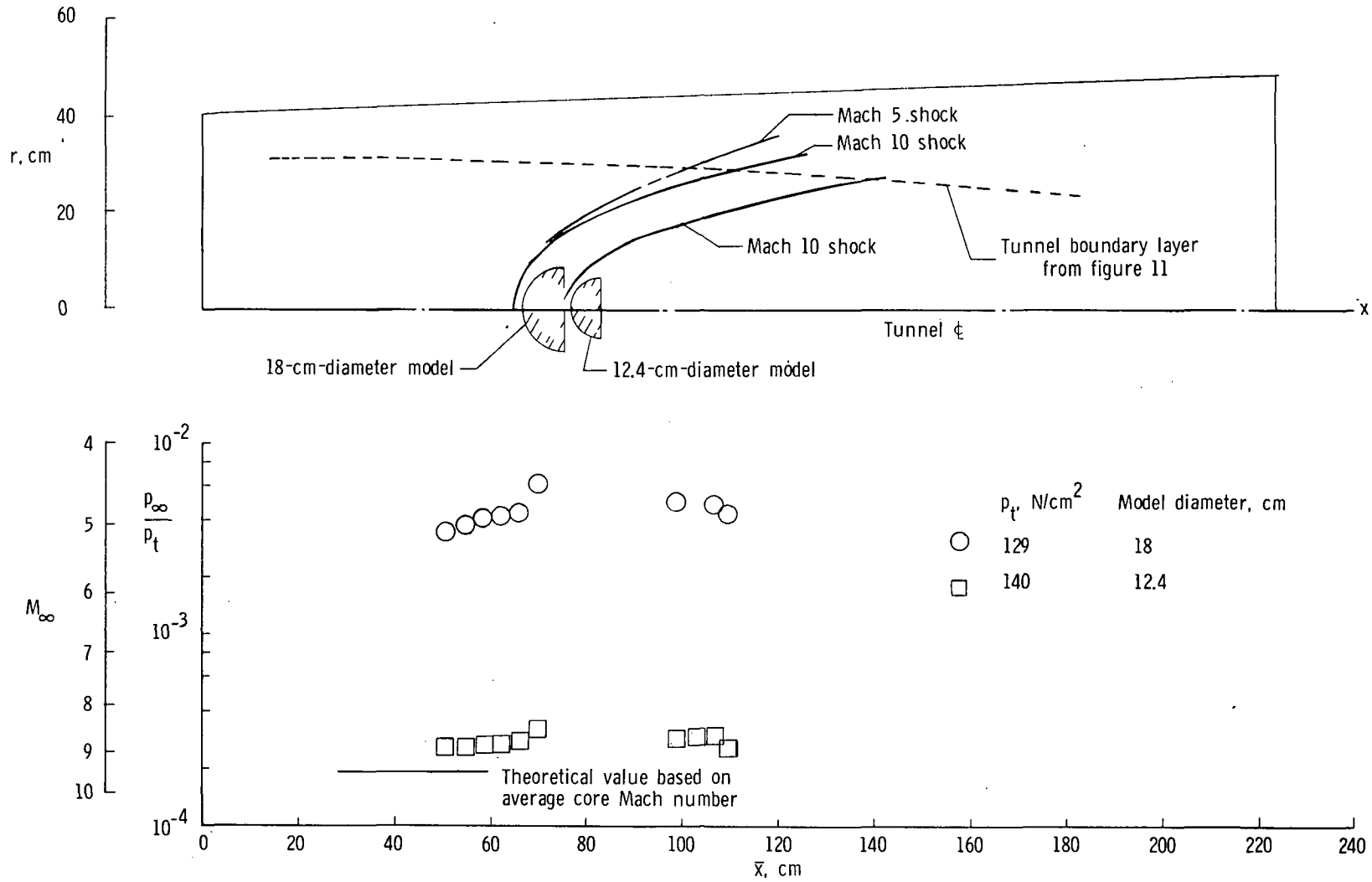

Figure 13.- Blockage test in Mach 10 tunnel.

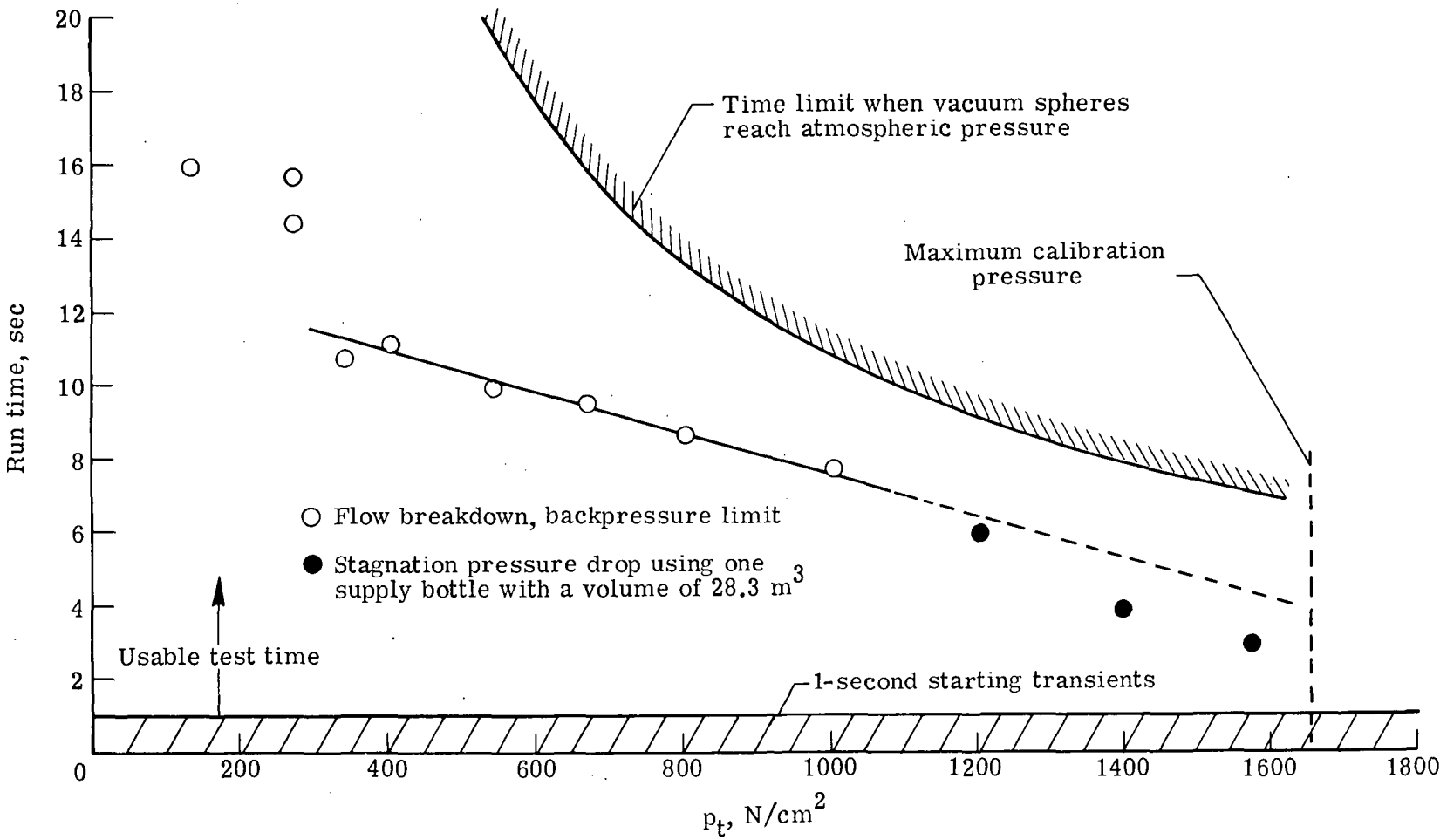

Figure 14.- Mach 10 tunnel run time.

NATIONAL AERONAUTICS AND SPACE ADMINISTRATION
WASHINGTON, D.C. 20546

OFFICIAL BUSINESS
PENALTY FOR PRIVATE USE $300

SPECIAL FOURTH-CLASS RATE
BOOK

POSTAGE AND FEES PAID
NATIONAL AERONAUTICS AND
SPACE ADMINISTRATION
451

U.S.MAIL

POSTMASTER : If Undeliverable (Section 158 Postal Manual) Do Not Return

"The aeronautical and space activities of the United States shall be conducted so as to contribute . . . to the expansion of human knowledge of phenomena in the atmosphere and space. The Administration shall provide for the widest practicable and appropriate dissemination of information concerning its activities and the results thereof."

—NATIONAL AERONAUTICS AND SPACE ACT OF 1958

NASA SCIENTIFIC AND TECHNICAL PUBLICATIONS

TECHNICAL REPORTS: Scientific and technical information considered important, complete, and a lasting contribution to existing knowledge.

TECHNICAL NOTES: Information less broad in scope but nevertheless of importance as a contribution to existing knowledge.

TECHNICAL MEMORANDUMS: Information receiving limited distribution because of preliminary data, security classification, or other reasons. Also includes conference proceedings with either limited or unlimited distribution.

CONTRACTOR REPORTS: Scientific and technical information generated under a NASA contract or grant and considered an important contribution to existing knowledge.

TECHNICAL TRANSLATIONS: Information published in a foreign language considered to merit NASA distribution in English.

SPECIAL PUBLICATIONS: Information derived from or of value to NASA activities. Publications include final reports of major projects, monographs, data compilations, handbooks, sourcebooks, and special bibliographies.

TECHNOLOGY UTILIZATION PUBLICATIONS: Information on technology used by NASA that may be of particular interest in commercial and other non-aerospace applications. Publications include Tech Briefs, Technology Utilization Reports and Technology Surveys.

Details on the availability of these publications may be obtained from:

SCIENTIFIC AND TECHNICAL INFORMATION OFFICE

NATIONAL AERONAUTICS AND SPACE ADMINISTRATION

Washington, D.C. 20546